# Chapter 2
# Experimental Analysis of Rational Harmonic Mode-Locked Fiber Laser

In this chapter, we purpose to generate the optical pulse train with higher repetition rate than modulation frequency. This chapter is organized as following: Section 2-1 introduces the background of the actively mode-locked fiber laser and our experimental motivation. In Section 2-2, we explain the physics and working principle of the mode-locked laser from the fundamental mode-locking to further rational harmonic mode-locking. In Section 2-3, we demonstrate the experimental results of rational harmonic mode-locked fiber laser (RHMLFL), and realize the amplitude equalization of pulse train by nonlinear modulation method. Finally, we draw the conclusion in our experiments.

## 2-1 Introduction

The development of high capacity and high speed optical fiber communication is always the trend for research of the optical communication due to the requirements of telecommunication networks. Wavelength division multiplexing (WDM) and optical time-division multiplexing (OTDM) are the efficient ways to overcome the bottleneck of the electrical components. The generation of optical pulse train with low chirp, short pulsewidth, high repetition rate is the key technique for realizing ultra high speed OTDM and soliton communication. Gain-switched distributed feedback semiconductor laser (GS-DFB), distributed feedback semiconductor laser with electro-absorption modulator, actively mode-locked semiconductor laser (AML-SL) and actively mode-locked fiber laser (AML-FL) can all achieve this objective. Actively mode-locked fiber ring lasers are promising sources of high repetition rate transform-limited optical pulses and suitable for soliton transmission systems [7–12]. Compared with actively mode-locked semiconductor lasers, fiber lasers give high average optical power, generally produce shorter optical pulses with low chirp, offer greater flexibility for inclusion of intra-cavity elements, freedom from mechanical alignment, and the tuning range of the wavelength almost covers all the gain spectrum of the erbium doped fiber amplifier (EDFA). However, the stability of such pulses is crucial, and it has been investigated theoretically and experimentally [7–13].

There are several methods for generating pulse laser such as Q-switching and mode-locking. In recent years, mode-locking is a hot technique used to produce a periodic pulse train with high peak power and short pulsewidth by forcing the phases of the modes to maintain their relative values. Q-switching produces relatively broader optical pulses (~ 100 ns). In contrast, mode-locking can generate pulses shorter than 100 fs. The first mode-locking laser was demonstrated by Gürs and Müller [14] in a Ruby laser in 1964. Gürs and Müller incorporated an internal modulator into the laser cavity to generate their pulse laser is referred to as active mode-locking. The modulator is driven by an external periodic wave to let the phase of the multi modes to be locked in frequency domain, and it forms a periodic pulse train in time domain. In the same year, the mechanism of mode-locking was first explained by DiDomenico and Yariv [15]. Another method, the passive mode-locking was then introduced in 1967 by Mocker and Collin [15]. A saturable absorber was used to suppress low intensity pulses in ruby lasers and enhance high lasing intensity.

In early experiments, the actively mode-locked laser generated broader optical pulse. The pulsewidth of > 1-ns produced by Nd-doped fiber lasers in 1986[16]. In 1988, pulse with full-width-half-maximum (FWHM) of 120 ps was obtained by using a pumping laser-diode array [17]. In 1989, many laboratories started to focus on the development of mode-locked $Er^{3+}$ doped fiber lasers (MLEDFLs), because of their potential applications in lightwave system [18-20].

Recently, harmonic mode-locked fiber laser has attracted great interest due to its ability to produce stable optical pulse train with very short pulsewidth and high repetition rate.

## 2-2 Physics of Active Mode-Locking

A laser may oscillate in many modes simultaneously, hence its output may consist of light of a number of frequencies. The frequency spacing among the modes is given by $\Delta\nu = c/L$, where $L$ is the one round trip length inside the cavity. In a general continuous wave multi-mode laser, the modes will oscillate independently of each other and will have random phases relative to one another. If the phases are locked in such way that there is a constructive interference between the modes at an instant and a destructive interference at other times, the output will appear as a pulse.

The electromagnetic field due to 2n+1 equally spaced modes is given by:

$$E(t) = \sum_{q=-n}^{n} E_q e^{i[(w_0 + q\Delta w)t + \varphi_q]} \quad (2\text{-}1)$$

where we have summed over all possible modes. $E_q$ is the amplitude of the $q$ th mode, $w_o$ is the frequency of a central mode, $\Delta w$ is the frequency spacing between modes, and $\varphi_q$ is the phase of the $q$ th mode. If all modes operate independently with random phase relationship among them, the interference terms in the total intensity $|E(t)|^2$ averages canceling to zero.

When mode-locking occurs, phases of various longitudinal modes are synchronized such that the phase difference between any two neighboring modes is locked to a constant value $\phi$ such that $\varphi_q - \varphi_{q-1} = \varphi$. In the case of equal amplitudes ($E_o$) and locked phases ($\varphi_q - \varphi_{q-1} = \varphi$), considered here, this sum becomes:

$$E(t) = E_0 e^{iw_0 t} \sum_{q=-n}^{n} e^{iq\Delta wt} \tag{2-2}$$

Then, it can be written as

$$E(t) = A(t) e^{iw_0 t} \tag{2-3}$$

where $A(t) = E_0 \sum_{q=-n}^{n} e^{iq\Delta wt}$ (2-4)

Therefore we have obtained an amplitude-modulated wave oscillating at the central mode frequency. In fact, the expression for $A(t)$ contains a geometrical progression. From this, we can convert it to another form and write down the intensity as a function of time in the following way:

$$I(t) \propto [A(t)]^2 = \frac{\sin^2[(2n+1)\Delta wt/2]}{\sin^2[\Delta wt/2]} \tag{2-5}$$

The laser output forms a pulse train whose individual pulses are spaced by $\Delta t$. $\Delta t$ is the round trip time inside the laser cavity. Every time the pulse reaches the output coupler, then a single pulse emitting, so that a regular pulse train is generated.

The pulsewidth of the mode-locked laser can be obtained from Eq. (2-5) to be $\Delta t = 2\pi[(2n+1)\Delta w]^{-1} = 1/\Delta \upsilon$, where $\Delta \upsilon$ is a FWHM of the generation band. we can find that the pulsewidth inversely proportions to spectral bandwidth. From this simple example, it becomes clear that mode-locking results in a periodic intensity pulse, in contrast to the output of the non-mode-locked case.

Consider a continuum of oscillating modes with non-equal amplitude distribution. This is an efficient approximation for real ultrashort pulse lasers, where there is very large number of closely spaced oscillating modes and their amplitude distribution usually forms a gaussian-like profile.

In the case the expression for $A(t)$ must be written as

$$A(t) = \sum_{q=-n}^{n} E_q e^{iq\Delta wt} \tag{2-6}$$

Then we put Eq. (2-6) into integral, and the limits may be taken to be infinity. The amplitude $E_n$ is appropriately zero in the limits:

$$A(t) = \int E_q e^{iq\Delta wt} dq \tag{2-7}$$

This integral is a Fourier transform. So, in the time domain the amplitude of a multi-mode output is given by the transform of the amplitude distribution of modes in the frequency domain. For example, the mode-locking of a continuum of oscillating modes with a gaussian distribution of amplitude will result in gaussian pulses:

$$[A(t)]^2 \approx \exp[-\ln 2(\frac{2t}{\Delta t_{0.5}})^2] \quad (2\text{-}8)$$

The duration of the half maximum of such pulses is given by:

$$\Delta t_{0.5} = \frac{2\ln 2}{\pi \Delta \nu} = \frac{0.441}{\Delta \nu} \quad (2\text{-}9)$$

In principle, the relation between the pulse duration and the width of oscillating spectra is:

$$\Delta t = \frac{k}{\Delta \nu} \quad (2\text{-}10)$$

where $k$ is a factor of the spectrum shape. However, this is valid provided that the mode-locking is considered for the simple phase relationship as $\varphi_q - \varphi_{q-1} = const$. In this case, generated pulses are called "transform limited pulses". The duration of such pulses is minimum and which is possible for a given optical spectrum of a pulse.

There are several techniques used to achieve mode-locking. In general, these techniques rely on some forms of periodic amplitude modulation of the multi-mode laser. If the modulation period corresponds to the round-trip time around the cavity $T = \frac{2L}{c}$ or, by other words, the modulation frequency corresponds to the allowed mode spacing between cavity longitudinal modes, the phenomenon of mode-locking can occur. The process leading to mode-locking can be explained both in the time domain and the frequency domain. In the frequency domain, we can consider that all the involved modes under modulation develop individual sidebands. These sidebands overlap with the neighboring modes, leading to the phase-locking of longitudinal modes to its neighbors. Practically, the methods of achieving mode locking can be split into two main techniques: active mode-locking and passive mode-locking.

## 2-2-1 Fundamental Mode-Locking

Active mode-locking requires amplitude or phase modulator driven by radio frequency at a frequency $f_m$ equal to or a multiple of the mode spacing $\Delta\upsilon$ . It is referred to as amplitude modulation (AM) or frequency modulation (FM) mode-locking depending on whether amplitude or phase modulator is used to generate pulses at the modulation frequency $f_m$, where:

$$f_m = f_c\,,\ \ f_c = \frac{c}{2nL} \qquad (2\text{-}11)$$

Here, $f_c$ is the cavity mode-spacing frequency, $c$ is the speed of light, $L$ is the cavity length and $n$ is the refractive index of the cavity. These pulses have a round trip time of $t_p$, which is related to $f_c$ and the pulsewidth by Eq. (2-11)

$$t_p = \frac{2nL}{c} \tag{2-12}$$

$$N = \frac{t_p}{\tau} \tag{2-13}$$

*N* is the total number of longitudinal modes in the cavity [21]. This is known as fundamental mode-locking, and it produces pulses at a repetition rate equal to $f_c$.

One can understand the locking process in frequency domain. Both the AM and FM techniques generate modulation sidebands, spaced apart by the modulation frequency $f_m$. These sidebands overlap with the neighboring modes when modulation frequency $f_m$ is equal to mode spacing $\Delta\upsilon$. Such an overlap leads to phase synchronization. Then, it forms a series of periodic pulse train in time-domain.

Taking the simplest case of sinusoidal modulation for example, assuming the modulating signal is:

$$a(t) = A_m \sin(\frac{1}{2}\omega_m t) \tag{2-14}$$

$A_m$ is the amplitude of the modulating signal, and $\omega_m$ is the angular frequency. The transmittance of the modulator is:

$$T(t) = T_0 + \Delta T_0 \cos(\omega_m t) \qquad (2\text{-}14)$$

$T_0$ is the average transmittance, and $\Delta T_0$ is the variable amplitude of transmittance.

Assuming the optical field before modulating is:

$$E(t) = E_c \sin(\omega_c t + \varphi_c) \qquad (2\text{-}16)$$

After modulating, the optical field in the cavity becomes:

$$E(t) = E_c T(t) \sin(\omega_c t + \varphi_c) = E_c[T_0 + \Delta T_0 \cos(\omega_m t)]T(t)\sin(\omega_c t + \varphi_c)$$
$$= A_c[1 + m\cos(\omega_m t)]\sin(\omega_c t + \varphi_c)$$

(2-17)

$A_c = E_c T_0$ is the amplitude of the optical field, and $m = \dfrac{E_c \Delta T_0}{A_c}$ is the modulation index of the modulator.

After expending Eq. (2-17), we can obtain:

$$E(t) = A_c \sin(\omega_c t + \varphi_c) + \frac{1}{2} m A_c \sin[(\omega_c + \omega_m)t + \varphi_c]$$
$$+ \frac{1}{2} m A_c \sin[(\omega_c - \omega_m)t + \varphi_c]$$

(2-18)

From Eq. (2-18), we can see the spectrum of the modulated optical field including three frequencies: $\omega_c$, upper sideband $(\omega_c + \omega_m)$, lower sideband $(\omega_c - \omega_m)$, and the phases of the three frequencies are equal. The process of sideband coupling leads to phase locking.

In other hand, the process of forming active mode-locking in time domain can be described as following. An acousto-optic or electro-optic modulator, a Mach-Zehnder integrated-optic modulators, or a semiconductor electroabsorption modulator incorporated in the laser cavity can be seen as a faster shutter. And, the shutter opens only for a very short period of time, every time the light pulse circles in the cavity. Instead of fully closing the shutter, shutter is modulated by the sinusoidal transmission. . A pulse with the right timing can pass the modulator at times where the losses are at a minimum. Still, the wings of the pulse experience a little attenuation, which effectively leads to pulse shortening in each round trip. It can be achieved by the modulation synchronized with the cavity round trips, and leads to the generation of ultrashort pulses.

## 2-2-2 Harmonic Mode-Locking

The most common technique for active mode-locking of fiber lasers makes use of an amplitude or phase modulator. Both acousto-optic and electro-optic modulators are good choices for active mode-locking. Nevertheless, most modulators with big size often cause large coupling losses when light passes through the modulator. $LiNbO_3$ modulators have the merits of compact size and small coupling losses are suitable for fiber system. And they can be operated at speeds as high as 40 GHz [22]. For these reasons, $LiNbO_3$ modulators are commonly used for mode-locked fiber lasers.

The cavity mode spacing frequency of a typical laser cavity is of the order of 0.5 ~ 5MHz. To increase the pulse repetition rate, pulses could be produced at integer harmonics of the cavity mode-spacing by modulating at a frequency $f_m$, given by:

$$f_m = pf_p \tag{2-19}$$

p(≦N) is an integer representing the number of longitudinal modes locked, and ranges from a few hundred to tens of thousand. This is known as harmonic mode-locking, and the new round trip time and its relationship with the pulsewidth is described in Eq. (2-20), (2-21):

$$t_p = \frac{2nL}{c} \cdot \frac{1}{p} \tag{2-20}$$

$$\frac{N}{P} = \frac{t_p}{\tau} \tag{2-21}$$

The Kuizenga and Siegman theory [23] predicts that with AM mode-locking the time bandwidth product is 0.44 for a chirp-free Gaussian pulse and 0.315 for a Sech pulse. Furthermore, it states that the pulsewidth $\tau$ is inversely proportional to $(\delta)^{1/4}$ and $(f_m \Delta f)^{1/2}$, so that:

$$\tau = K\left(\frac{1}{f_m \Delta f}\right)^{\frac{1}{2}}\left(\frac{1}{\delta}\right)^{\frac{1}{4}} \tag{2-22}$$

Here $\delta$ is the effective single-pass amplitude modulation depth, $\Delta f$ is the gain bandwidth of the laser cavity and $K$ is a pulse shape-dependent constant. Therefore, with increasing of the modulation frequency and modulation amplitude level, the pulsewidth of output can be shorter.

Harmonic mode-locked lasers that produce stable pulses up to repetition rates of 40GHz have been reported [24]. The cavity lengths needed to generate these pulses decrease rapidly with increasing repetition rates. Additionally, they require modulators and signal generators at the required repetition rate, increasing the cost and complexity of the system.

## 2-2-3 Rational Harmonic Mode-Locking

Actively mode-locked fiber lasers have the ability to generate continuous short pulse trains in a wide range of repetition rates; however, this range has been limited by the modulation bandwidth of modulators. Ahmed and Onodera [25] introduced the idea of mode-locking a laser cavity at rational harmonics of the modulator frequency, to generate pulses at a repetition rate higher than the modulator frequency. This is achieved by slightly detuning the modulator frequency $f_m$ by Eq. (2-23), (2-24) through the rational number *k,* which can have values ranging from 1 to no more than 20 [26,27]:

$$f_m = \left( p \pm \frac{1}{k} \right) \cdot f_c \tag{2-23}$$

where $f_c$ is the cavity frequency.

This leads to a pulse repetition rate of $f_p$, given by

$$f_p = (kp \pm 1) \cdot f_c \tag{2-24}$$

Therefore, rational harmonic mode-locked fiber lasers generate optical pulses at a repetition rate that is *k* times greater than the modulator frequency.

Rational harmonic mode-locking of erbium-doped fiber lasers at repetition rates up to 200GHz have been reported [28], using values of $k$ as high as 15, to generate pulse trains with a repetition rate many times that of the driving RF source. Following this method, we can use the synthesizer with a modulation frequency no higher then 2.7 GHz to generate pulse trains with repetition higher then 10 GHz.

The phenomenon of pulse repetition rate doubling and tripling in actively mode-locked lasers is caused by the interaction between circulating pulses and the cavity loss modulation [29]. The result of varying the RF drive frequency slightly is to induce phase shift. It is equal to delay the arrival of each pulse with respect to loss minimum. The relationship between the value of delay and detuning frequency is $T/k$, where $T$ is the modulation period. If each pulse is delayed by half of the modulation period $T$, then when it arrives at next time, it will pass through the modulator at loss maximum. Fig. 2-1 describes pulses circulating in the ring cavity when $k$ is 2. At first, pulse $A$ forms at the maximum transmission of the modulator, then the slight shift of the modulation frequency causes the pulse delay half modulation period, and pulse $B$ forms at the minimum transmission of the modulator. After one round trip, all the pulses delay half modulation period, so pulse $A$ experiences the minimum transmission of the modulator, and pulse $B$ sees the maximum transmission of the modulator. The pulse experiences the minimum transmission of the modulator will not extinguish, because the relaxation time of the gain medium is much longer than the pulse period [25].

The repetition rate tripling occurs in the same process. The frequency shift of $f_c/3$ of the modulation frequency cause the pulses in the cavity are delayed by $T/3$ when they pass the modulator every round trip. Fig. 2-2 shows the timing diagram of pulses circulating in the ring cavity when $k$ is 3. We can see every pulse will experience the same transmission of the modulator after $k$ round trips. We can also understand the amplitude fluctuation of frequency troubling is more serious than the case of frequency doubling. This indicates that the higher $k$ leads the laser more unstable. When $k \geqq 3$, different pulses experience different losses in the modulator [25]. The scheme of the rational harmonic mode-locked laser causes frequency multiplication, however it also accompanies the unequal amplitude of the pulse train [28,29]. These fluctuations greatly increase the bit error rate, and therefore are not tolerable in optical communication systems. But, this problem does not exist for k=2.

# 2-3 Experimental Analysis of Rational Harmonic Mode-Locked Fiber Laser

In rational harmonic mode-locked fiber lasers, the optical modulator is the determining component for locking the harmonics of the resonant spectrum into a particular longitudinal mode. For this reason, it is very important to characterize the optical modulator. We measure and find the biasing and optical transmission transfer characteristics of the Mach-Zehnder interferometric modulator. First, we use the MZI modulator operating in linear region. With properly detuning the modulation frequency and polarization state, we can get the eighth order of rational harmonic optical pulse train with repetition rate up to 20 GHz, which is eight times of modulation frequency 2.5 GHz. But, the amplitude of the pulse train is not equal because of the mismatch of lower order harmonics. We proposed to solve the problem by using nonlinear modulation of modulator without adding any other components. And we can get the optical pulse train of equal amplitude up to fourth rational harmonic order with repetition rate of 10 GHz.

## 2-3-1 Measurement of MZI modulator transmission function

The experimental setup for measuring the MZI modulator transmission function is shown in Fig. 2-3. The tunable laser HP 8168F is fed to the input of the MZI modulator through a polarization controller. Because the MZI modulator is sensitive to the polarization state, the fiber polarization controller (PC) is used to rotate the input polarization of the light coupled properly to the diffused channel waveguide of the interferometric intensity modulator of MZI modulator. The MZI modulator is the JDS Uniphase amplitude modulator (modal no. 21014025), whose bandwidth is 40 GHz. The 50Ω termination is used for matching the RF traveling waves and has no effect in this measurement. The output of the MZI modulator is connected to an optical power meter (Advantest modal. No. Q8221) to measure the output power. The MZI modulator transmission characteristic is measured at 1530nm, and the output power of the laser source is set at 0 dBm. Table. 2-1 shows the output powers of the MZI modulator at different values of the bias voltage $V_{bias}$, and we can determine the following parameters of the modulator:

$$V_{\pi} = V_{biasMax} - V_{biasMin} = 3.8 - (-0.4) = 4.2V \qquad (2\text{-}25)$$

*Extinction ratio:* $P_{outMax} - P_{outMin} = (-5.8) - (-25.6) = 19.8dB$ (2-26)

Insertion loss : $P_{in} - P_{outMax} - L_{pc} = 0 - (-5.8) - 1 = 4.8dB$ (2-27)

where $V_{biasMax}$ is the bias voltage applied to obtain maximum output power; similarly the $V_{biasMin}$ is for minimum output power, $L_{pc}$ : Polarization controller insertion loss. The normalized optical transmittance (transmission function) of the modulator is defined as:

$$T = \frac{I_o}{AI_I} = \frac{P_{out}}{P_{outMax}} \qquad (2\text{-}28)$$

where $I_o$ and $I_I$ are the output and input intensity respectively. $A$ is a constant accounted for the insertion loss of the modulator.

The measured and the theoretical $\cos^2$ fit transmission function of the MZI modulator are shown in Fig. 2-4. Hence the modulator transmission function can be approximated by a $\cos^2$ profile:

$$T = \cos^2\left(\frac{\pi(V_m - 3.8)}{2V_\pi}\right) = \cos^2\left(\frac{\pi(V_m - 3.8)}{8.4}\right) \quad (2\text{-}29)$$

$V_m$ is the bias voltage applied to MZI modulator.

## 2-3-2 Experimental Setup

The configuration of the laser is shown schematically in Fig. 2-5. The gain media of the ring laser cavity is provided by an erbium-doped fiber amplifier (Lightwave Link, 19"Rack mount, model no. EDFA-1700H). The output power of the EDFA is 17dBm. And there are two isolators incorporated in the erbium-doped fiber amplifier to ensure the unidirectional operation of the ring laser. A Mach-Zehnder modulator (JDS Uniphase, modal no. 21014025) is used as a mode-locker offering intracavity periodic loss modulation, which is biased at the quadrature point with a voltage of 1.6 V and then driven by superimposing a sinusoidal signal with amplitude level of 15 dBm derived from a 2.7 GHz synthesizer (Leader, modal no. 3221). The laser could be forced to operate stably at harmonic frequencies of the cavity fundamental mode by tuning the modulation frequency. Because of the somewhat polarization dependent of the modulator, a polarization controller is placed before the modulator to adjust the polarization state of the light for improving the modulation efficiency. Power is coupled out of the cavity with a 90:10 fiber coupler, where 90% of the total power is used as feedback to the cavity, and 10% is extracted out from the cavity. The output spectral and temporal characteristics are measured with an optical spectrum analyzer (Anritsu, modal no. MS9710C) with 0.05 nm resolution, a high speed digital sampling oscilloscope (Agilent, 86100A) and a 50GHz photodiode (Discovery Semiconductors, DSC10S) together with an electronic spectrum analyzer (HP, 8565E).

When the polarization controller is correctly adjusted, then various orders of rational harmonic mode-locking can be obtained by only tuning the modulation frequency.

## 2-3-3 Analysis of Results

Fig. 2-6 shows the amplified spontaneous emission of erbium-doped fiber amplifier. The erbium-doped fiber is used as the gain medium. By absorbing the 980 nm pumping laser, it can generate wide-band light source, and the peak value of the wavelength is 1530 nm. This causes the central wavelength of the laser we generate is 1530 nm.

The fundamental cavity frequency we measure is $f_c$=5.15 MHz as shown in Fig. 2-7. Following formula of the free spectral range (FSR): $FSR = \frac{c}{nL}$, where n is 1.46, the $c$ is velocity of light and $L$ is the cavity length, we can derive the cavity length is 39.89m. It corresponds to the cavity length 40m we measured. The average power of the output is 5.35 dBm. Initially, the frequency of modulation $f_m$ is adjusted to be an exact multiple of the natural frequency of the cavity, forcing the laser to operate in the region of harmonic mode-locking in the frequency of the modulator.

The laser is mode-locked by supplying a +15dBm RF signal, and the modulation frequency is set at 2.51842530 GHz which is equivalently equal to 489 times of $f_c$, harmonic mode-locking laser pulse is obtained at the output as shown in Fig. 2-8. The interval between adjacent pulses is about 400 ps, corresponding to a repetition rate of 2.5 GHz. The pulsewidth is also measured by the sampling oscilloscope, and $T_{FWHM}$ is 37 ps. The output pulse amplitude can be measured, and an average power is recorded at 3.42 mW. The peak power is 36.973 mW. The locked pulses are formed with clear pedestal, with slightly fluctuated amplitude.

Fig. 2-9 shows the optical spectrum of the output pulses. The 3dB bandwidth (*BW*) is 0.098 nm with the peak wavelength at 1530.398 nm. According to the relationship of time-bandwidth from Fourier transform, we can understand that when we succeed in mode-locking, the bandwidth of output will be much wider than operating in CW region. Fig. 2-10 shows the optical spectrum of operating in CW region, the *BW* of the optical spectrum is 0.039 nm. When mode-locking occurs, the optical spectrum becomes wider shown as Fig. 2-8. The 3dB bandwidth of the optical spectrum is 0.098 nm.

The bandwidth product (TBP) is calculated as:

$$TBP = T_{FWHM} \times BW \qquad (2\text{-}29)$$

Thus, we can obtain the TBP as 0.464. The pulses generated from AM mode-locked fiber laser are nearly transform-limited [30-32]. This means that the TBP takes the value of 0.44, assuming Gaussian shape pulse. We observe the RF spectrum of the pulse at the output of the fast photodiode both in wideband and narrowband illustrated on Fig. 2-11 and Fig. 2-12. The peak at 2.5 GHz again confirms the laser is locked at the repetition rate of 2.5 GHz. In order to get stable pulses, fine tuning of the RF frequency and polarization controller are necessary. The sidemode suppression ratio (SMSR) of the 2.5 GHz can be observed in narrowband of RF spectrum is 31.5 dB.

To obtain higher repetition rate the rational harmonic mode-locking (RHML) technique should be used. The phenomenon of RHML is observed when the modulation frequency is varied according to the relationship $f_m = \left(p \pm 1/k\right) \cdot f_c$. The modulation frequency is not an integer number harmonic of the fundamental frequency $f_c$ but detuned by an amount of $f_c / k$. The output pulse repetition rate is now no longer $f_m$ but $kf_m$. In another word, it has been multiplied by $k$. The pulse is then obtained by careful tentative tuning of the modulation frequency $f_m$ around the value calculated from this expression.

## 2-3-3-1 5 GHz Pulse Train Generation

Fig. 2-13 shows the output pulse train of the rational harmonic mode-locked laser when the modulation frequency is set to 2.52100037

GHz, that is equal to $f_c + f_c / 2$ and the modulator is biased with a voltage of 1.6V . The pulsewidth of 33.4 ps FWHM is obtained. The pulse period is 200 ps which correspond to a repetition rate of 5 GHz. It means the repetition rate is double. Fig. 2-14 shows the optical spectrum of the output pulses. The FWHM bandwidth is 0.1 nm with the peak wavelength at 1531.978 nm. The RF spectrum of the pulse illustrated on Fig. 2-15 is also confirmed the doubling repetition rate. We also observe the harmonic tune of more high frequency in the RF spectrum. The SMSR is measured as shown in Fig. 2-16, and the value is 27.67 dB.

## 2-3-3-2 7.5 GHz Pulse Train Generation

Fig. 2-17 shows the output pulse train of the rational harmonic mode-locked laser when the modulation frequency is set to 2.52014201 GHz, that is equal to $f_c + f_c / 3$, and the modulator is biased with a voltage of 1.6V. The pulsewidth of 30 ps FWHM is obtained. The pulse period is 133 ps which correspond to a repetition rate of 7.5 GHz. It means the repetition rate is triple. Fig. 2-18 shows the optical spectrum of the output pulses. The FWHM bandwidth is 0.13 nm with the peak wavelength at 1530.0672 nm. The RF spectrum of the pulse illustrated on Fig. 2-19 is also confirmed the tripling repetition rate, and the SMSR is measured as shown in Fig. 2-20, and the value is 23.66 dB.

## 2-3-3-3 10 GHz Pulse Train Generation

Fig. 2-21 shows the output pulse train of the rational harmonic mode-locked laser when the modulation frequency is set to 2.51971284 GHz, that is equal to $f_c + f_c / 4$, and the modulator is biased with a voltage of 1.6V. The pulsewidth of 26 ps FWHM is obtained. The pulse period is 100 ps which correspond to a repetition rate of 10 GHz. The repetition rate is four time of the modulation frequency. Fig. 2-22 shows the optical spectrum of the output pulses. The FWHM bandwidth is 0.136 nm with the peak wavelength at 1529.5294 nm. We can observe the spectrum have a separation of 0.08 nm, which corresponds to a longitudinal mode separation of 10 GHz. The RF spectrum of the pulse illustrated on Fig. 2-23 is also confirmed the four time of repetition rate. The SMSR is measured as shown in Fig. 2-24, and the value is 22.5 dB.

## 2-3-3-4 15 GHz Pulse Train Generation

Fig. 2-25 shows the output pulse train of the rational harmonic mode-locked laser when the modulation frequency is set to 2.51928366 GHz, that is equal to $f_c + f_c / 6$, and the modulator is biased with a voltage of 1.6V. The pulsewidth of 22.7 ps FWHM is obtained. The pulse period is 67 ps which correspond to a repetition rate of 15 GHz. It means the repetition rate is six time of the modulation frequency. Fig. 2-26 shows the optical spectrum of the output pulses. The FWHM bandwidth is 0.173 nm with the central wavelength at 1530.634 nm. The RF spectrum of the pulse illustrated on Fig. 2-27 is also confirmed the six time repetition rate. The SMSR is measured as shown in Fig. 2-28, and the value is 15.83 dB.

#### 2-3-3-5 20 GHz Pulse Train Generation

Fig. 2-29 shows the output pulse train of the rational harmonic mode-locked laser when the modulation frequency is set to 2.51906907 GHz, that is equal to $f_c + f_c/8$, and the modulator is biased with a voltage of 1.6V. The pulsewidth of 19.5 ps FWHM is obtained. The pulse period is 50 ps which correspond to a repetition rate of 20 GHz. It means the repetition rate is eight time of the modulation frequency. Fig. 2-30 shows the optical spectrum of the output pulses. The FWHM bandwidth is 0.18 nm with the central wavelength at 1530.024 nm. The RF spectrum of the pulse illustrated on Fig. 2-31 is also confirmed the eight time of repetition rate. The SMSR is measured as shown in Fig. 2-32, and the value is 13.5 dB.

### 2-3-4 Amplitude Equalization of Rational Harmonic Mode-locked Laser

With generation of higher order harmonics, the pulse train suffers serious uneven amplitude. The large amplitude fluctuation is caused by unmatched lower order harmonics distorting the pulse amplitude. Uneven amplitudes in an optical pulse train give rise to difficulties in the real application of the laser. There are many kinds of method developed to overcome the difficulty. In 1998, Jeon used the laser cavity composed of the nonlinear amplifying loop mirror (NALM) and farady rotator mirror (FRM) to realize the amplitude equalization of the fifteenth order rational harmonic mode-locked laser[33]. Besides, a SOA loop mirror[34], nonlinear polarization rotation (NPR)[35], an external fiber laser-based pulse amplitude equalization scheme[36], and letting the pulse pass through the amplitude modulator twice is also demonstrated[37]. However, above methods need to add additional photonic component to let the amplitude equalize. This may cause extra insertion loss in the cavity and cost higher. Here, we realize the pulse amplitude equalization by tuning the bias voltage applied to the MZI modulator to let the modulator operate in the nonlinear region to suppress the lower order harmonics in the cavity. This method doesn't need to add additional optical component and is effective for our rational harmonic mode-locked laser.

## 2-3-4-1 Principle

The transfer function of the modulator can be shown as [38]:

$$T(t) = (1-\alpha)\{1+\sin[\pi(b+M\cos(2\pi f_m t))]\} \tag{2-30}$$

where

$$b = (V_b - 1.6) / V_\pi \tag{2-31}$$

is the normalized bias point of the modulator we use, and

$$M = V_{ac} / V_\pi \tag{2-32}$$

is the normalized amplitude of the modulating signal. A bias voltage of 1.6V corresponds to a central point of the linear region of the MZI modulator transfer characteristic. $\alpha$ is the insertion loss, and $f_m$ is the frequency of the microwave drive signal. Eq. (2-30) shows the transfer function of the modulator can have varied shape by selecting different *b* and *M*. For an arbitrary rational harmonic order, if we can properly choose the value of *b* and *M*, the pulses circulating in the ring cavity will experience the same value of transmission in every round trip. Thus, the amplitude level of the output pulse train is equalized by the nonlinear modulation.

## 2-3-4-2 Experimental Result

Fig. 2-17, 2-21, and 2-25 show the optical pulse train with unequal amplitude. Fig. 2-19, 2-23, and 2-27 illustrate the RF spectrum of the beat signal corresponding to the third, fourth and sixth-order rational harmonic mode-locked fiber ring laser individually. If the lower order harmonics are not suppressed, they will make pulse train with unequal amplitude.

With properly tuning the bias voltage of modulation frequency and polarization controller, we can obtain the optical pulse train with equal amplitude as shown in Fig. 2-33, 2-35, and 2-38. And, we observe the lower harmonics are effectively suppressed. When b=0.4 and M=0.42, we can see the third-order harmonic frequency higher then the lower harmonic frequency from originally 13.5 dB without nonlinear modulation improving to 25.17 dB as shown in Fig.2-34. when b=1.5 and M=0.42, We can also see the fourth-order harmonic frequency higher then the lower harmonic frequency from originally 5.16 dB without nonlinear modulation improving to 19 dB as shown in Fig.2-36. Fig. 2-37 shows the transfer function of the modulator based on Eq. (2-30) for the fourth rational harmonic order.

From Fig.2-39, we can see the sixth-order harmonic frequency higher then the lower harmonic frequency from originally 5.84 dB without nonlinear modulation improving to 14.34 dB after using nonlinear modulation, when b=0.94 and M=0.42.

The amplitude equalization scheme is useful for third, and fourth order of rational harmonic mode-locked laser. But for sixth order and higher order of rational harmonic mode-locked laser, however we tune the bias voltage of modulator and polarization state, we can't get the equal amplitude pulse train from the output by this method. The effect of suppressing the lower harmonics is also decreasing when the rational harmonic order goes up.

## 2-4 Discussion and Summary

By changing the modulation frequency slightly, high order rational harmonic mode-locking has been achieved. In this section, we show a pulse oscillation as high as 2.5~20 GHz. Pulse trains are produced with repetition rates of 5, 7.5, 10, 15 and 20 GHz by detuning the modulation frequency from $pf_c = 2.5184253$ GHz by $f_c/2$, $f_c/3$, $f_c/4$, $f_c/6$, $f_c/8$. Fig 2-40 indicates the relationship between the pulsewidth of the generated pulse train of the RHMLFL and rational harmonic orders, we can observe that the pulsewidth decreases with increasing of the higher order of the RHMLFL. It corresponds to the result [39]

$$\tau_p = 2\times\sqrt{\frac{\ln 2}{\Gamma_0}}$$

$$= 4\sqrt{\ln 2}\times\frac{(p\cdot\alpha_m\cdot p_m)^{1/4}}{\sqrt{\omega_m\cdot\Delta\omega_a}}$$

$$\times\left[-\sum_{i=0}^{p-1}\sum_{j=0}^{i-1}\left(\frac{T''\big|_{t=\varphi_i}}{2T\big|_{t=\varphi_j}}+\frac{T'\big|_{t=\varphi_i}}{T\big|_{t=\varphi_i}}\cdot\frac{T'\big|_{t=\varphi_j}}{T\big|_{t=\varphi_j}}\right)\right]^{-1/4} \quad (2\text{-}36)$$

where p is the order of rational harmonic mode-locking, $\alpha_m\cdot p_m$ is the round trip gain coefficient, $\Delta\omega_\alpha$ is the linewidth of the laser medium combined with the optical bandpass filter inside the cavity, T is periodic over $2\pi$, $\omega_m$ is the modulation frequency, and $\varphi_i$ is the phase of the modulation when the pulse comes into the modulator for $i$th time . Fig 2-41 shows the relationship between the bandwidth of the generated pulse train of the RHMLFL and rational harmonic orders. Fig. 2-42 indicates the relationship between the SMSR of the generated pulse train of the RHMLFL and rational harmonic orders. In the condition of higher rational harmonic order, the modulation frequency becomes more and more critical, and the drift of the length of laser cavity caused by temperature changing will cause variation of the fundamental cavity frequency. Small change of the fundamental cavity frequency may cause the mismatch of the modulation frequency in high rational harmonic orders. So the SMSR of the mode-locked pulse obviously increases with the increase of rational harmonic order.

And we realize the amplitude equalization of the optical pulse train generated from a rational harmonic mode-locked fiber laser without adding any other additional optical components. Amplitude equalized short pulses up to the fourth order rational harmonic mode-locking are obtained with nonlinear modulation of the modulator and proper polarization state.

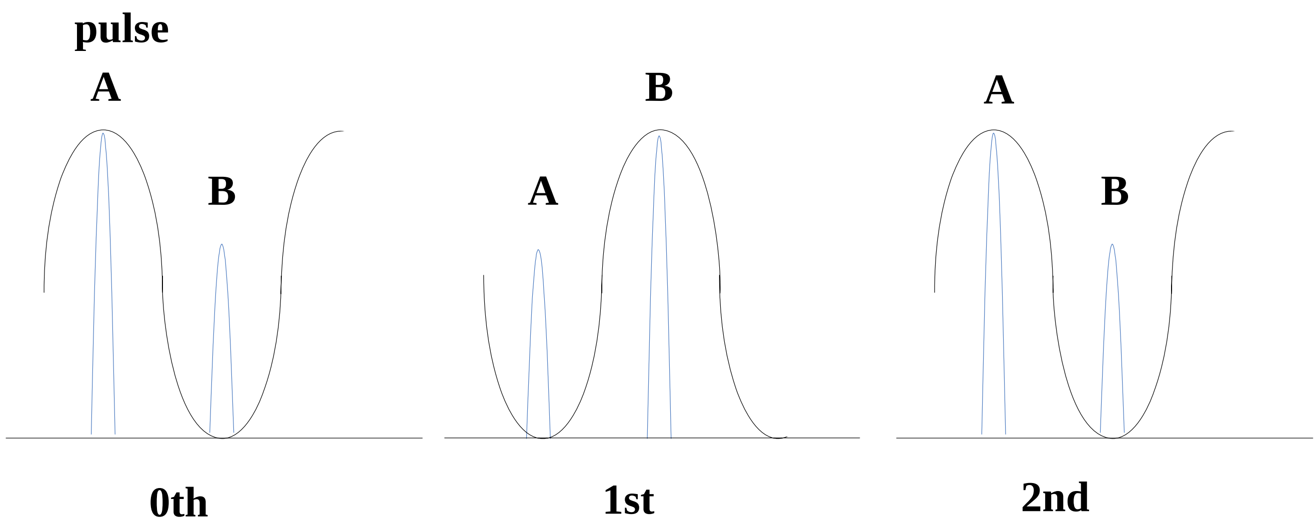


Figure. 2-1 Timing diagram of the pulse circulating in the ring cavity every round trip when $k = 2$.

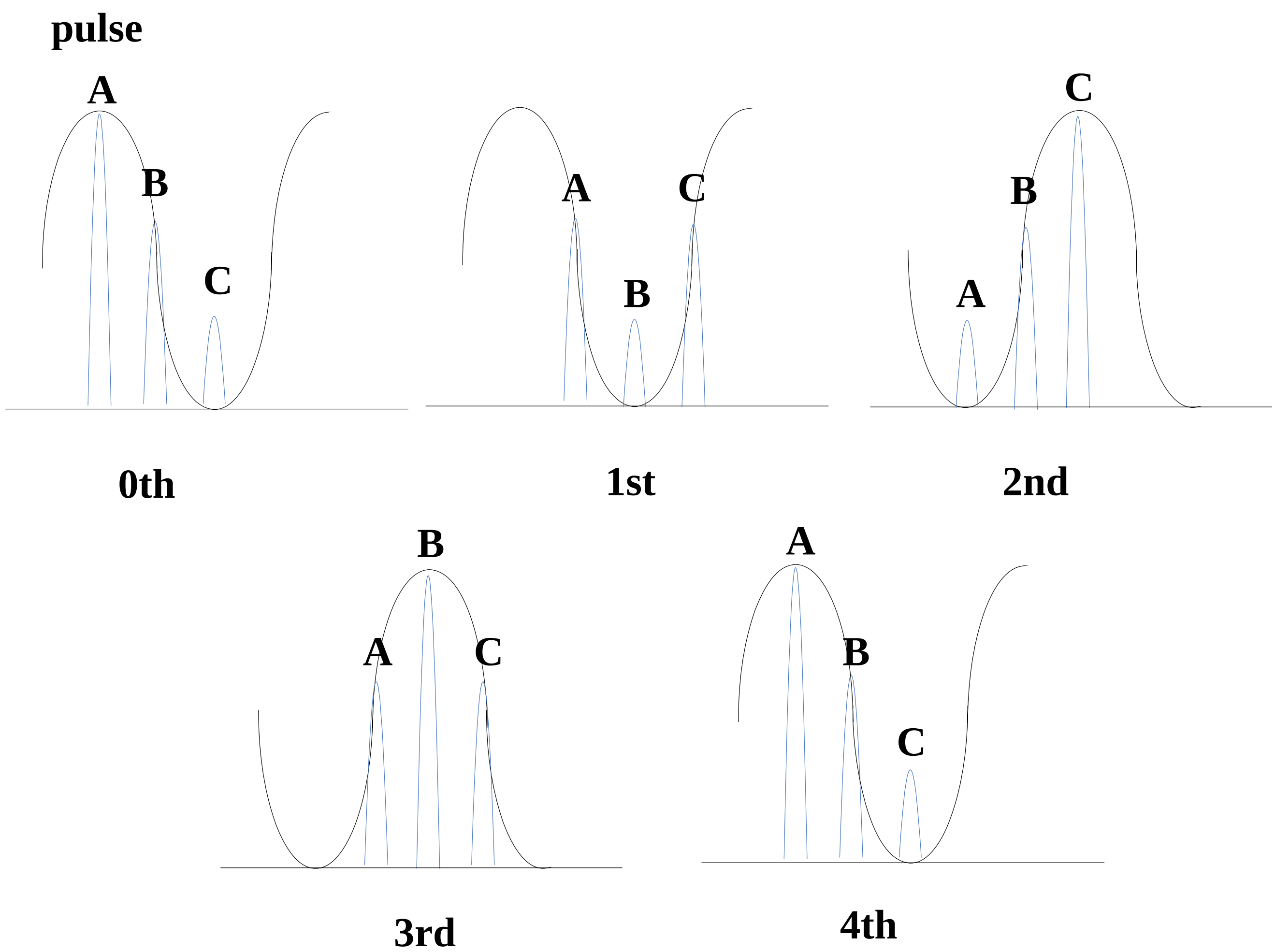


Figure. 2-2 Timing diagram of the pulse circulating in the ring cavity every round trip when $k = 3$.

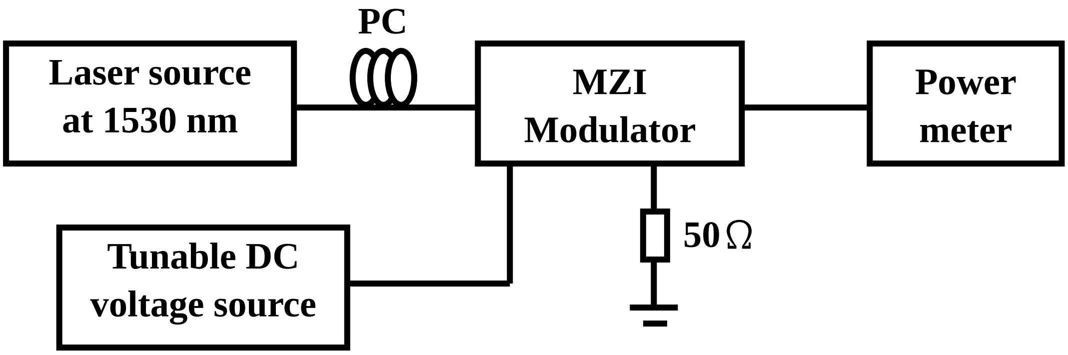


Fig. 2-3 The measurement setup of MZI modulator.

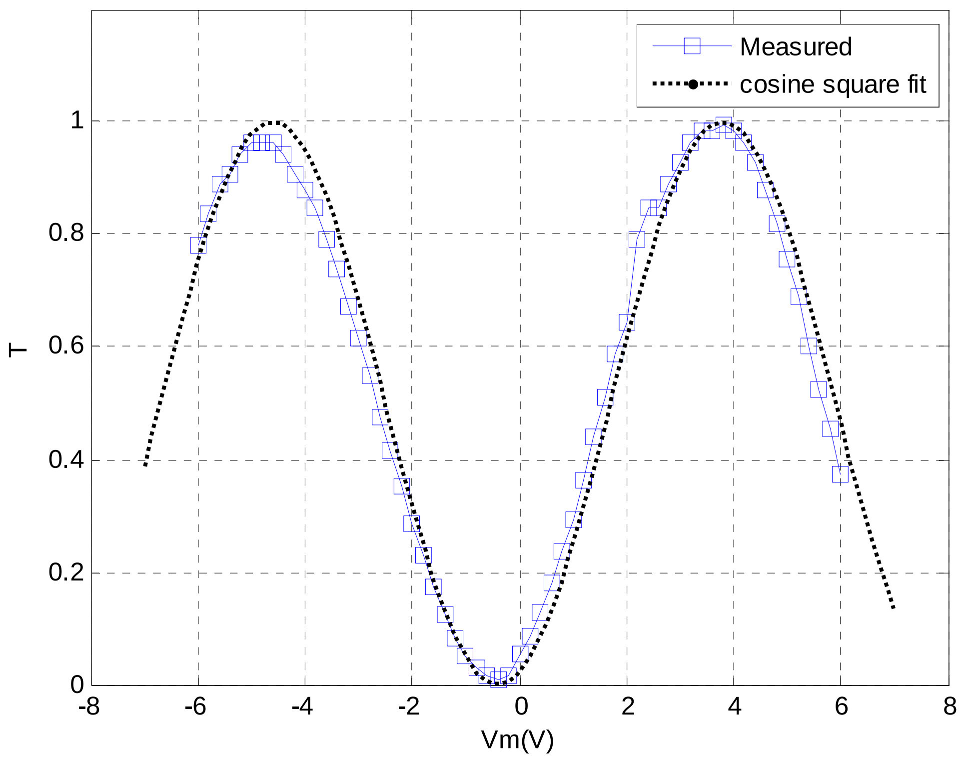


Fig. 2-4 MZI modulator normalized optical output intensity as a function of the DC voltage applied to the modulator.

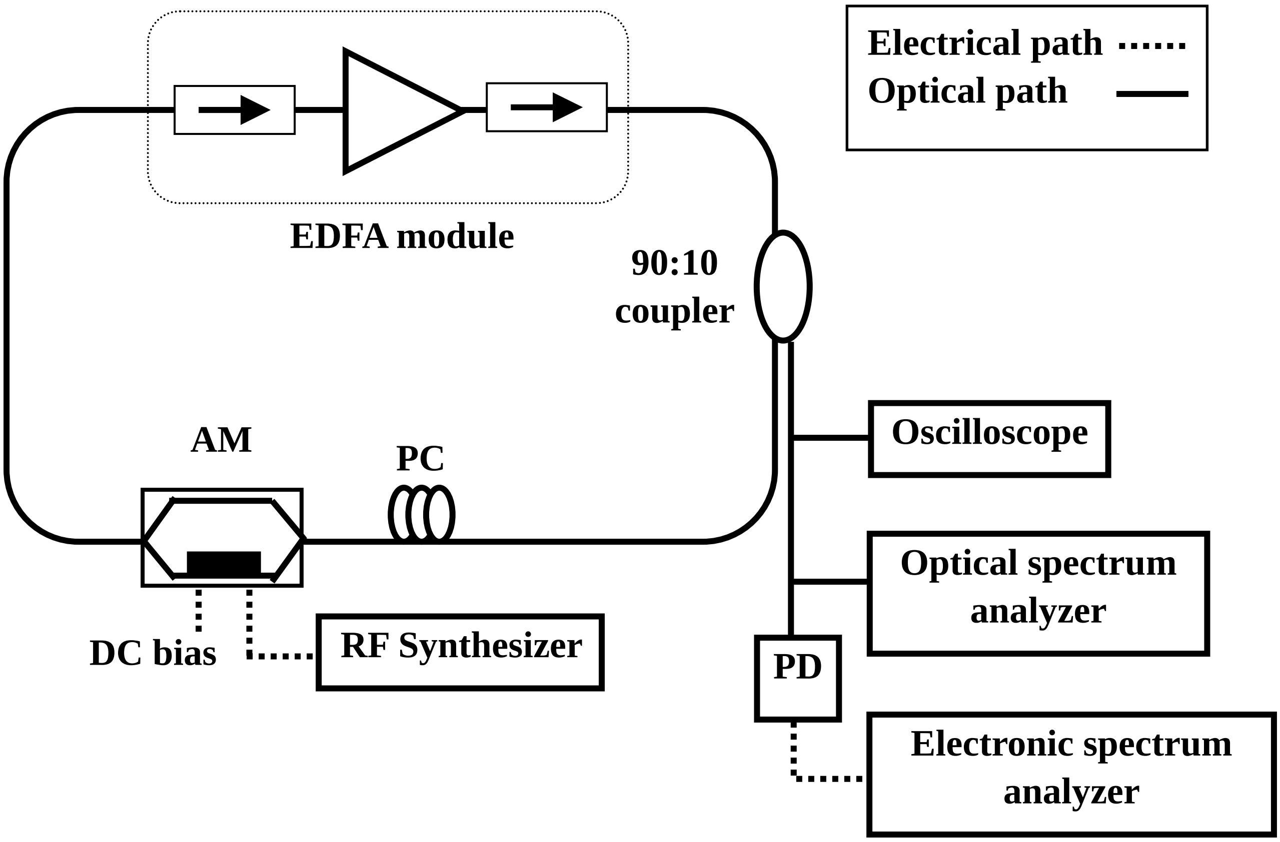


Fig. 2-5 The experimental setup of an amplitude-modulated MLFL.

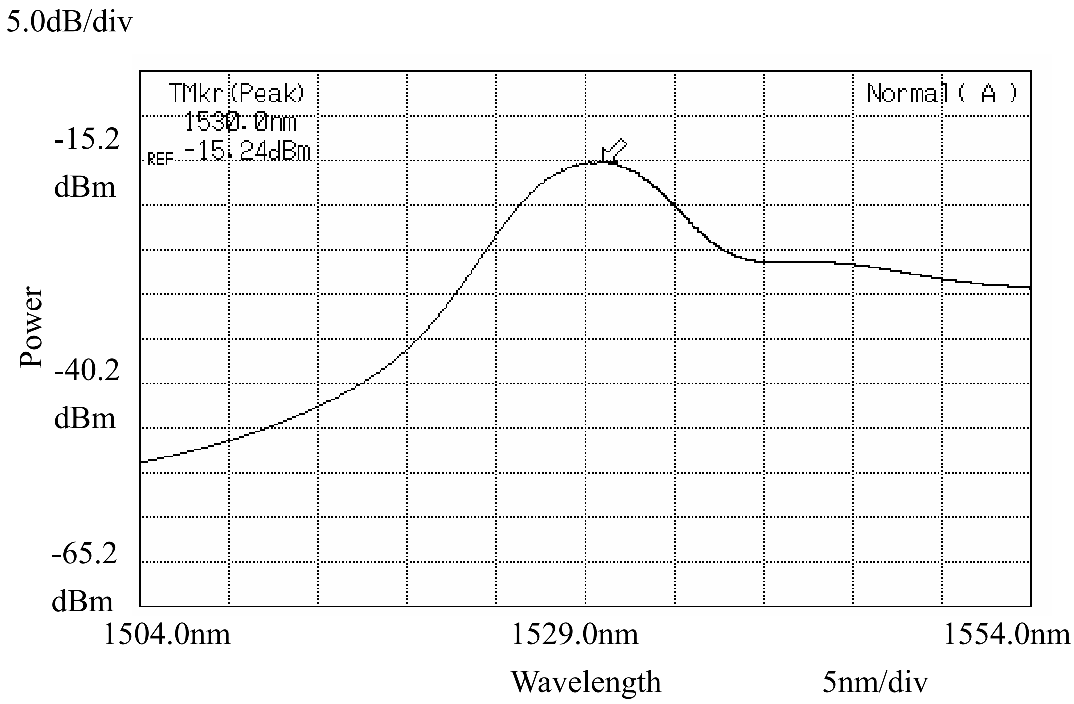


Fig. 2-6 Amplified spontaneous emission spectrum of EDFA.

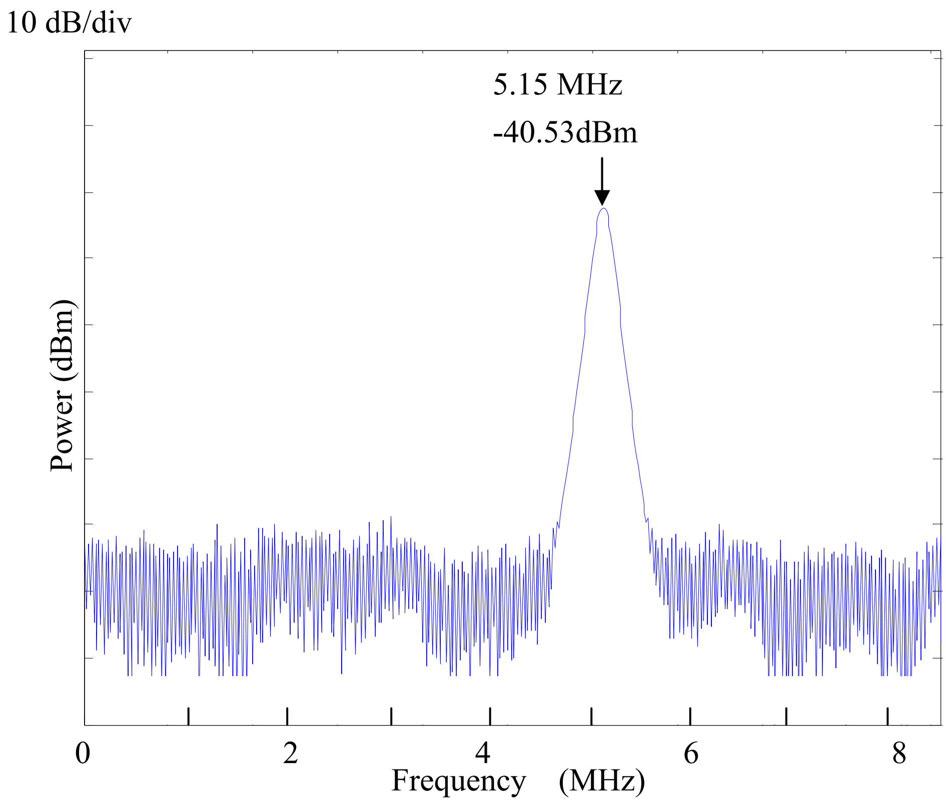


Fig. 2-7 Fundamental frequency of laser cavity.

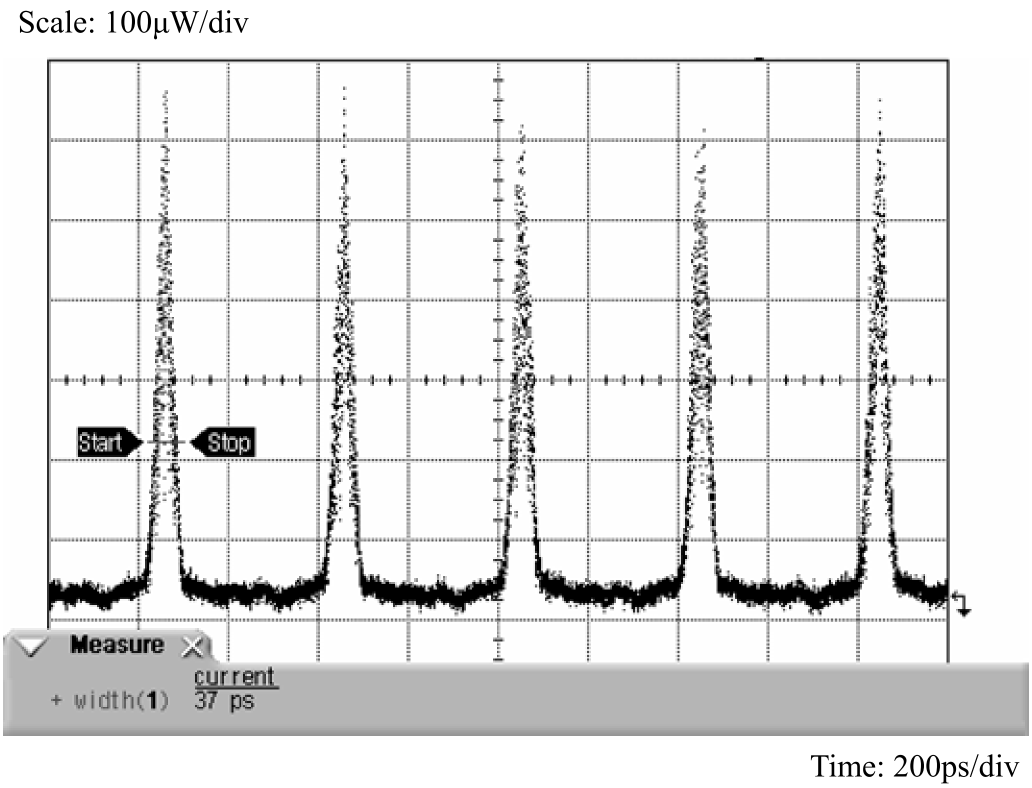


Fig. 2-8 Harmonic mode-locked pulse train with repetition rate of 2.5 GHz.

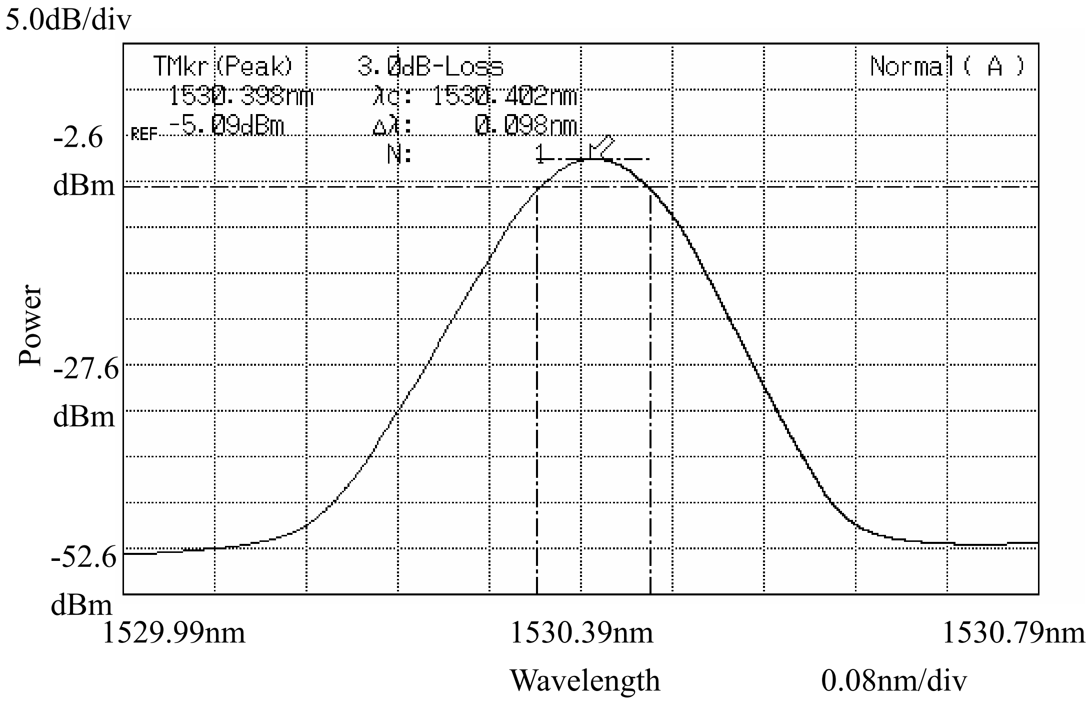


Fig. 2-9 Optical spectrum of harmonic mode-locked pulse train with repetition rate of 2.5 GHz.

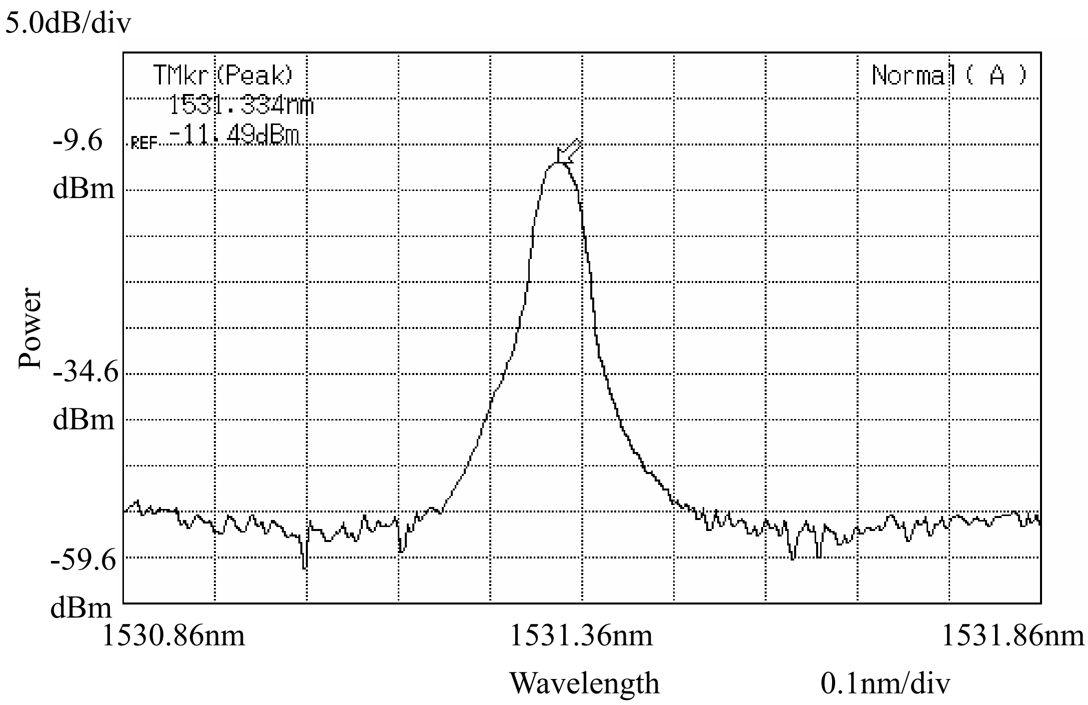


Fig. 2-10 Optical spectrum before mode locking.

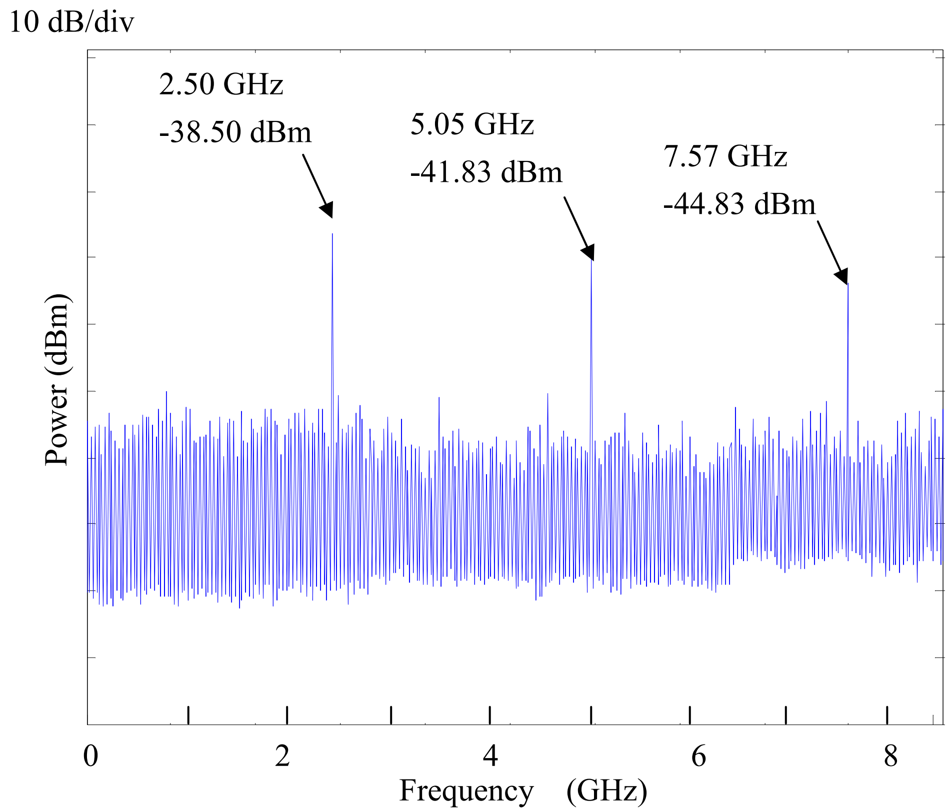


Fig. 2-11 RF spectrum(wideband) of harmonic mode-locked pulse train with repetition rate of 2.5 GHz.

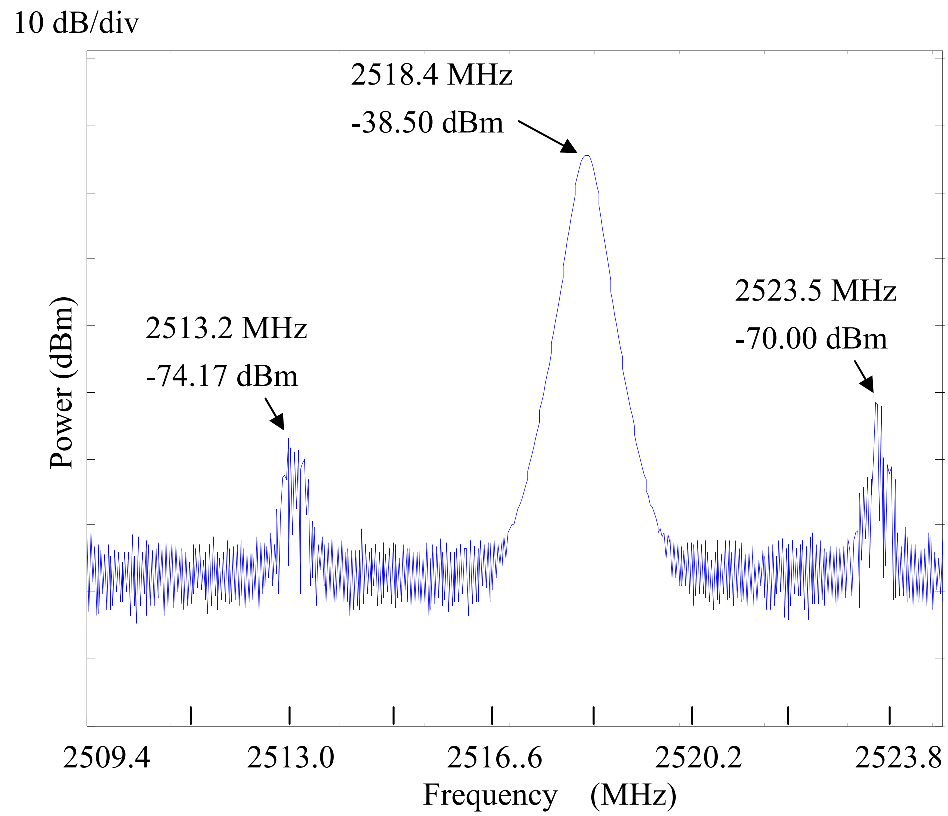


Fig. 2-12 RF spectrum(narrowband) of harmonic mode-locked pulse train with repetition rate of 2.5 GHz.

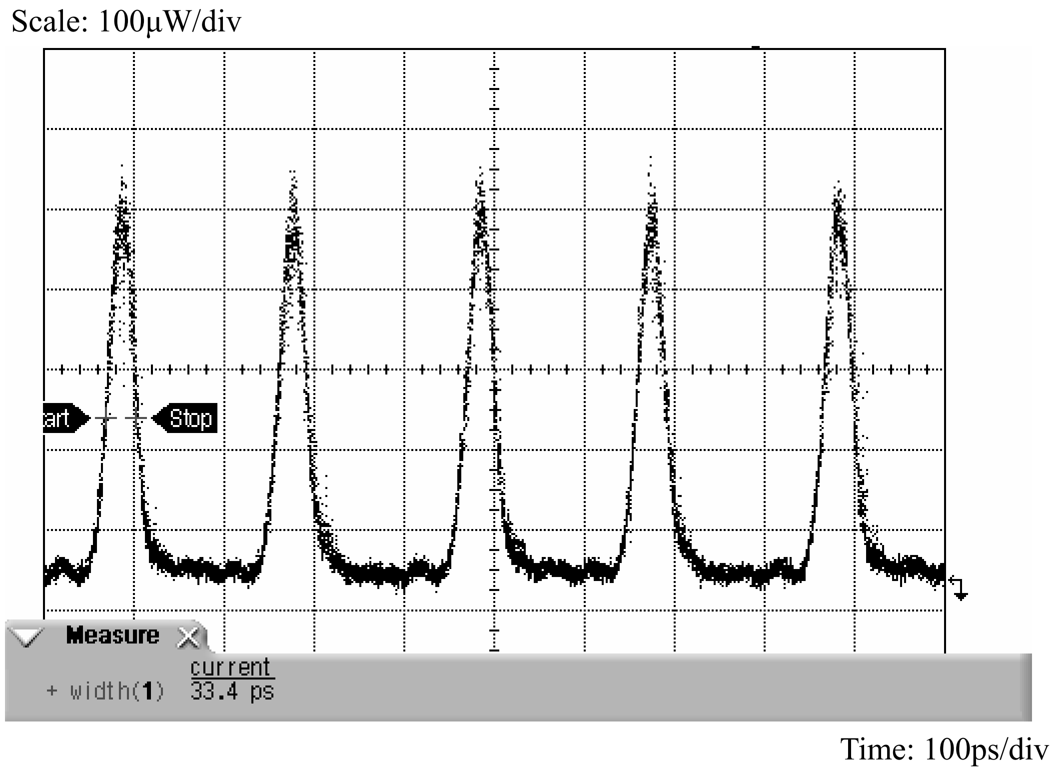


Fig. 2-13 Pulse train of RHMLFL with repetition rate of 5 GHz.

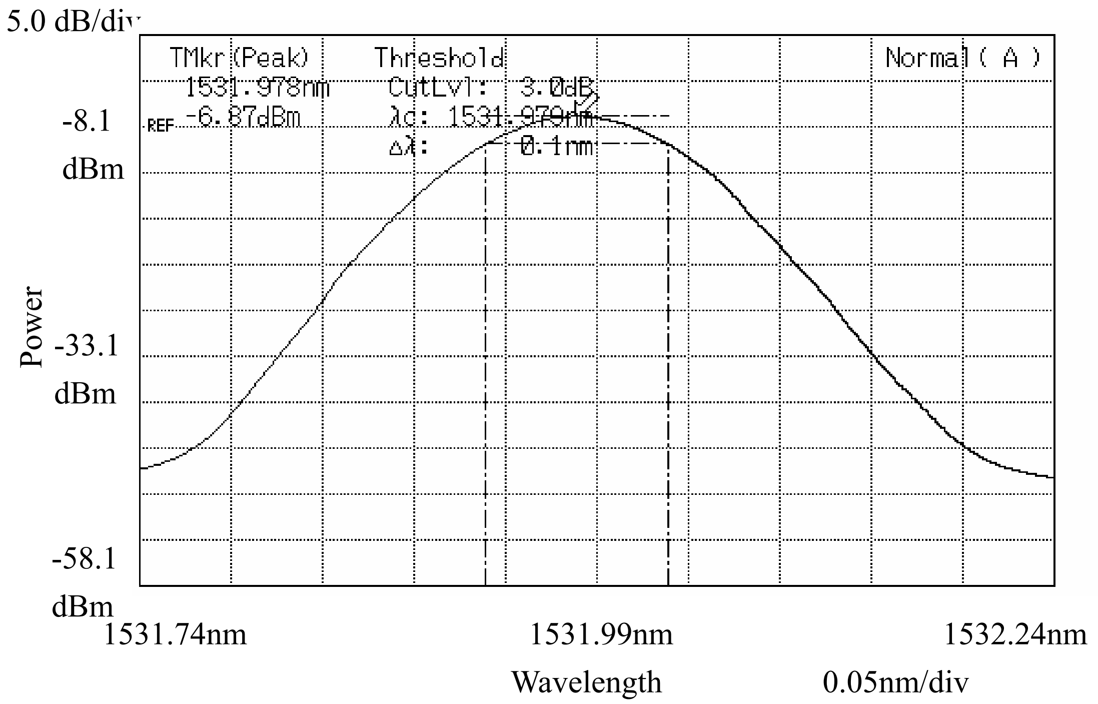


Fig. 2-14 Optical spectrum of RHMLFL with repetition rate of 5 GHz.

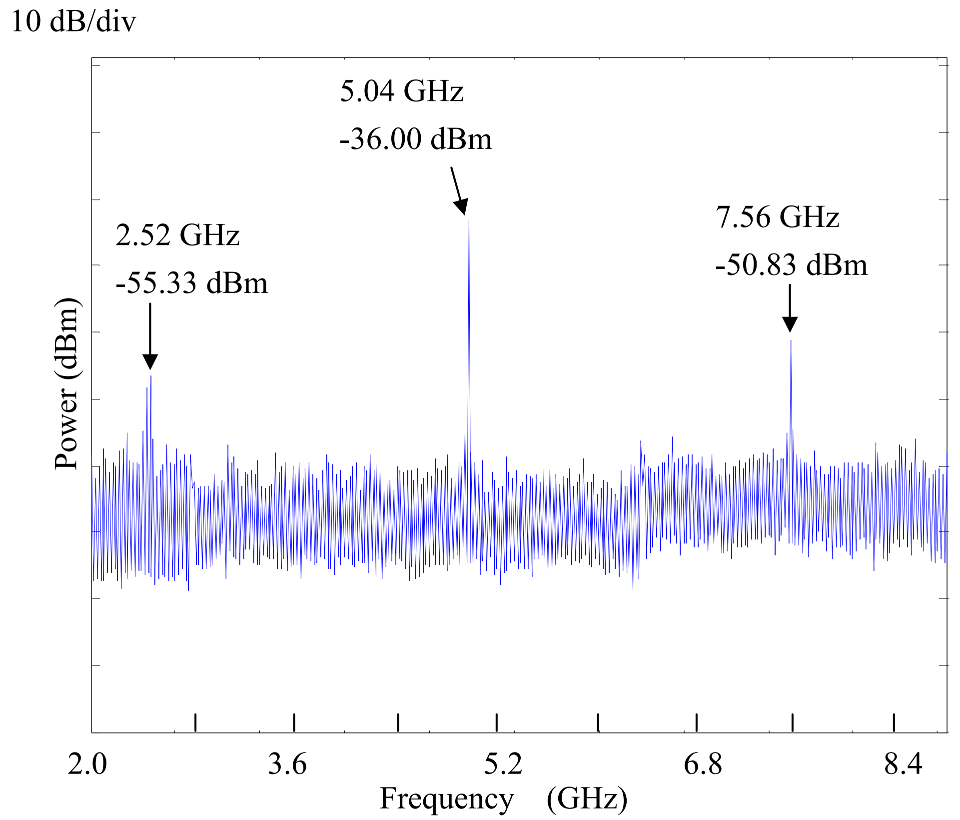


Fig. 2-15 RF spectrum(wideband) of RHMLFL with repetition rate of 5 GHz.

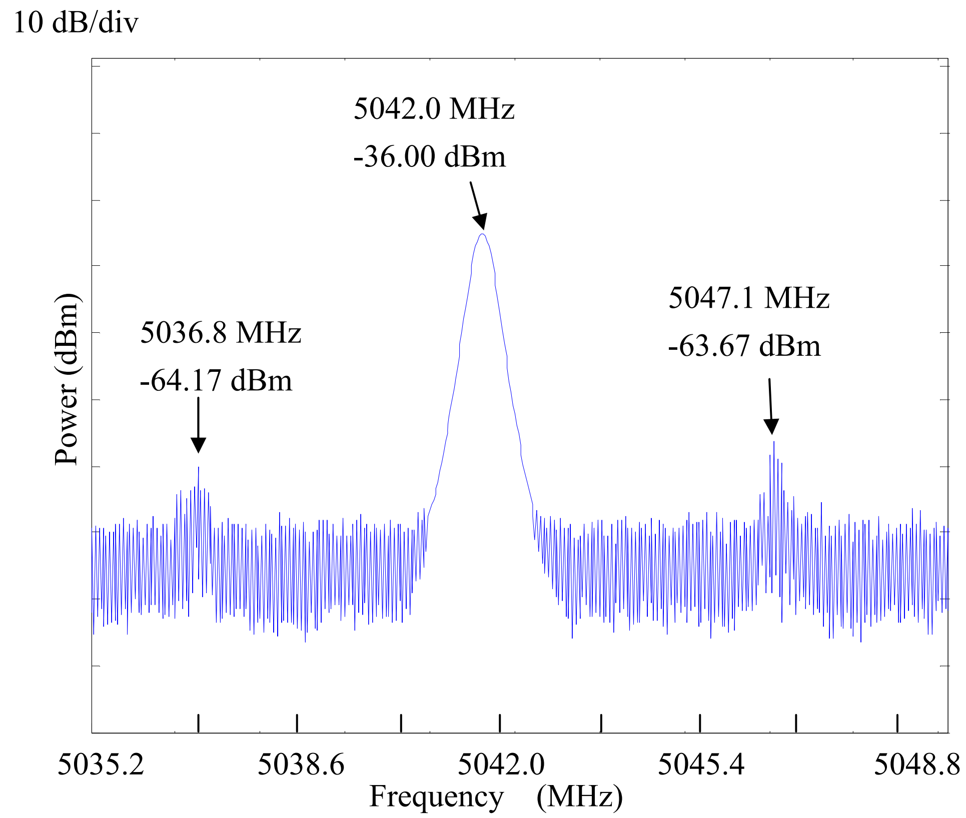


Fig. 2-16 RF spectrum(narrowband) of RHMLFL with repetition rate of 5 GHz.

Scale: 450µW/div

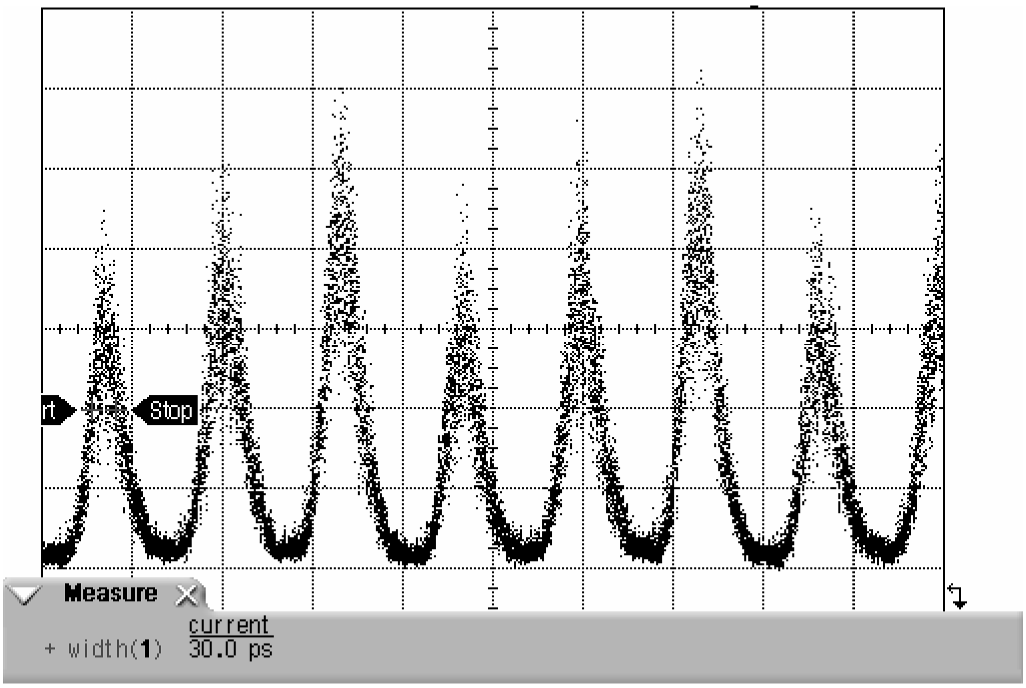


Time: 100ps/div

Fig. 2-17 Pulse train of RHMLFL with repetition rate of 7.5 GHz.

4.0dB/div

Power

-9.3 dBm

-29.3 dBm

-49.3 dBm

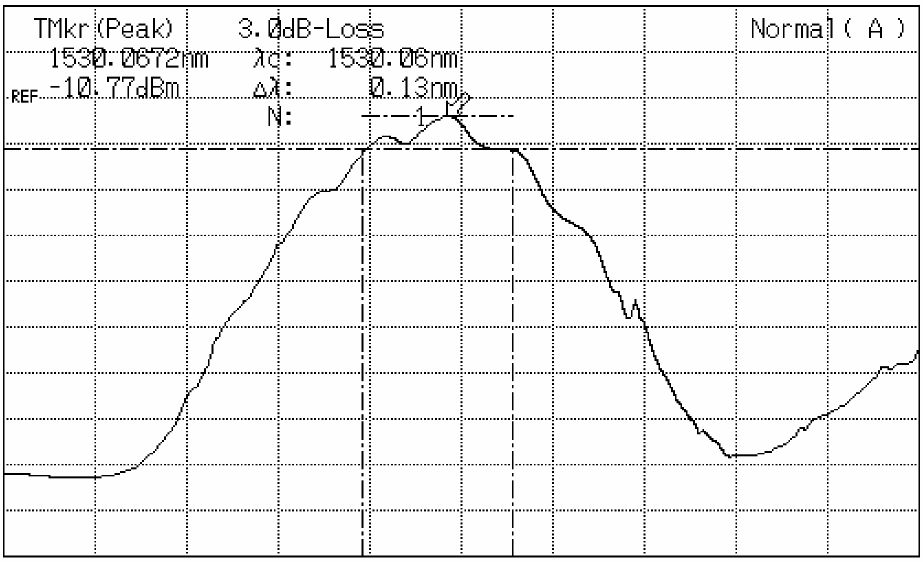


1529.68nm 1530.08nm 1530.48nm

Wavelength 0.08nm/div

Fig. 2-18 Optical spectrum of RHMLFL with repetition rate of 7.5 GHz.

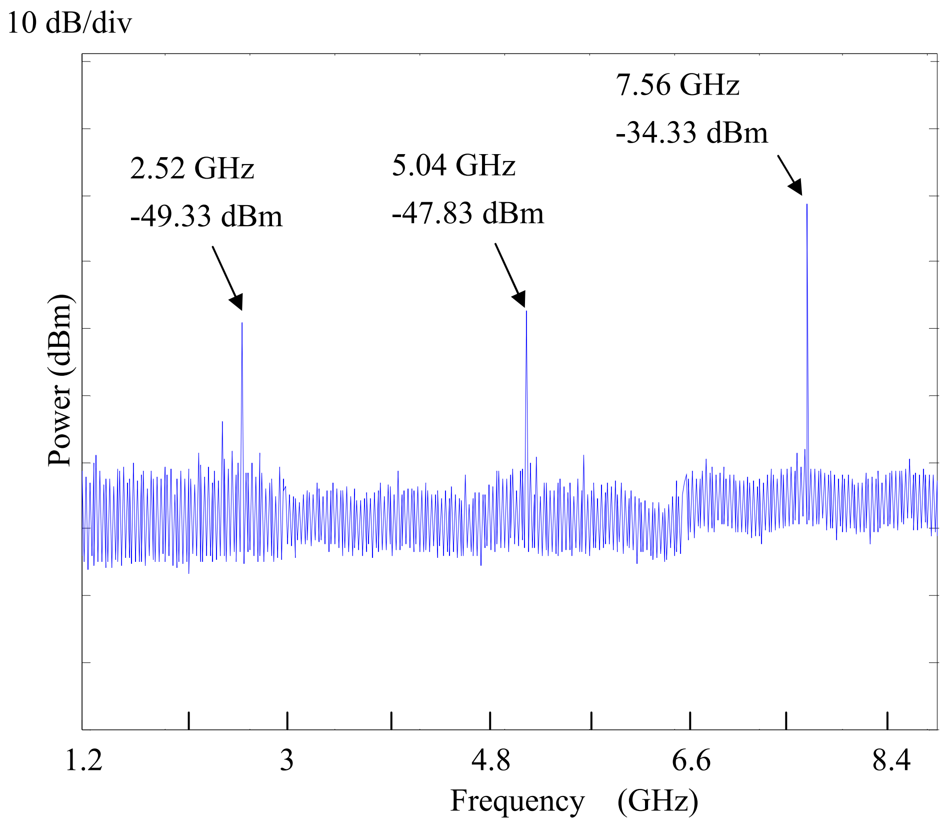


Fig. 2-19 RF spectrum(wideband) of RHMLFL with repetition rate of 7.5 GHz.

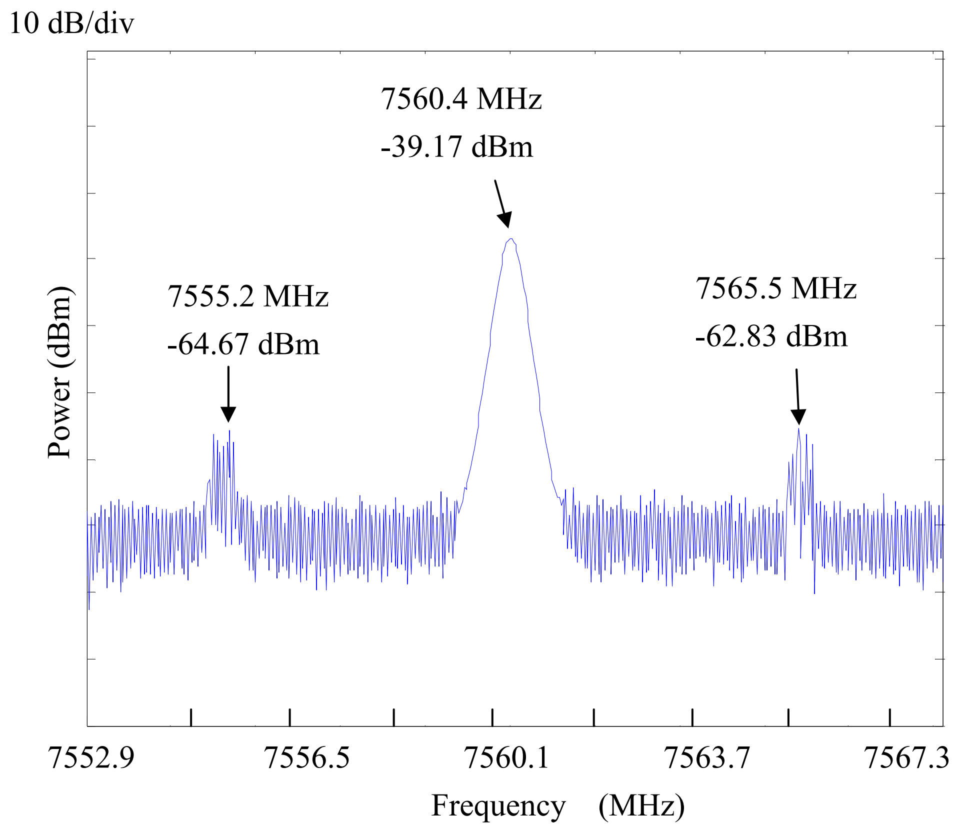


Fig. 2-20 RF spectrum(narrowband) of RHMLFL with repetition rate of 7.5 GHz.

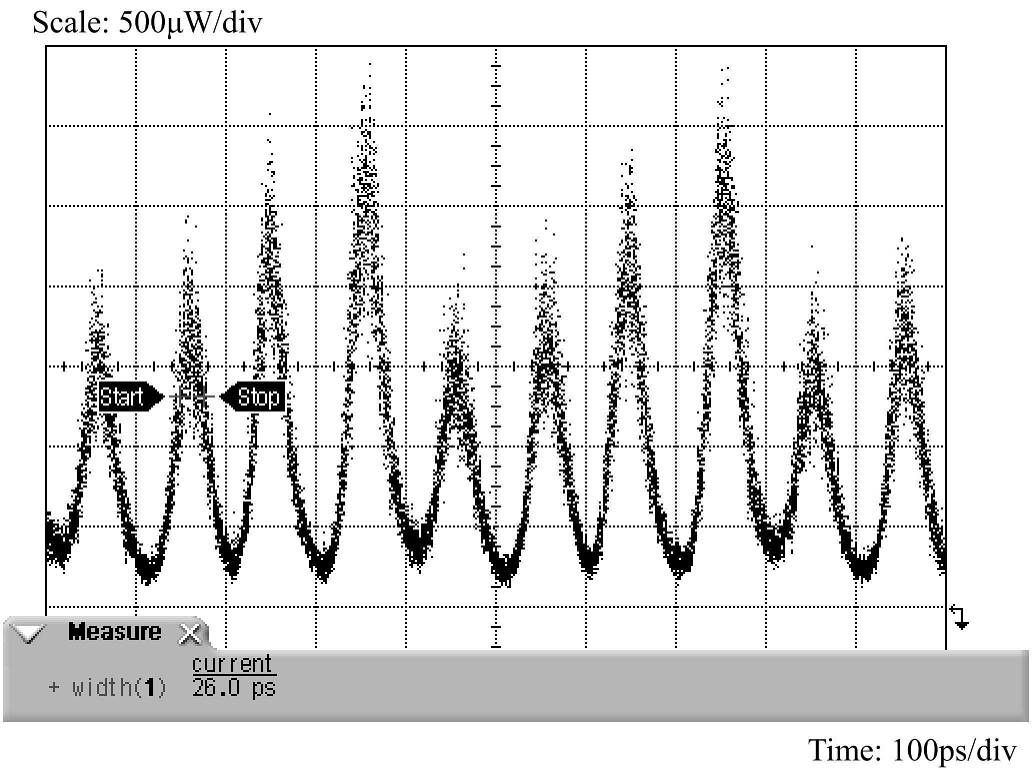


Fig. 2-21 Pulse train of RHMLFL with repetition rate of 10 GHz.

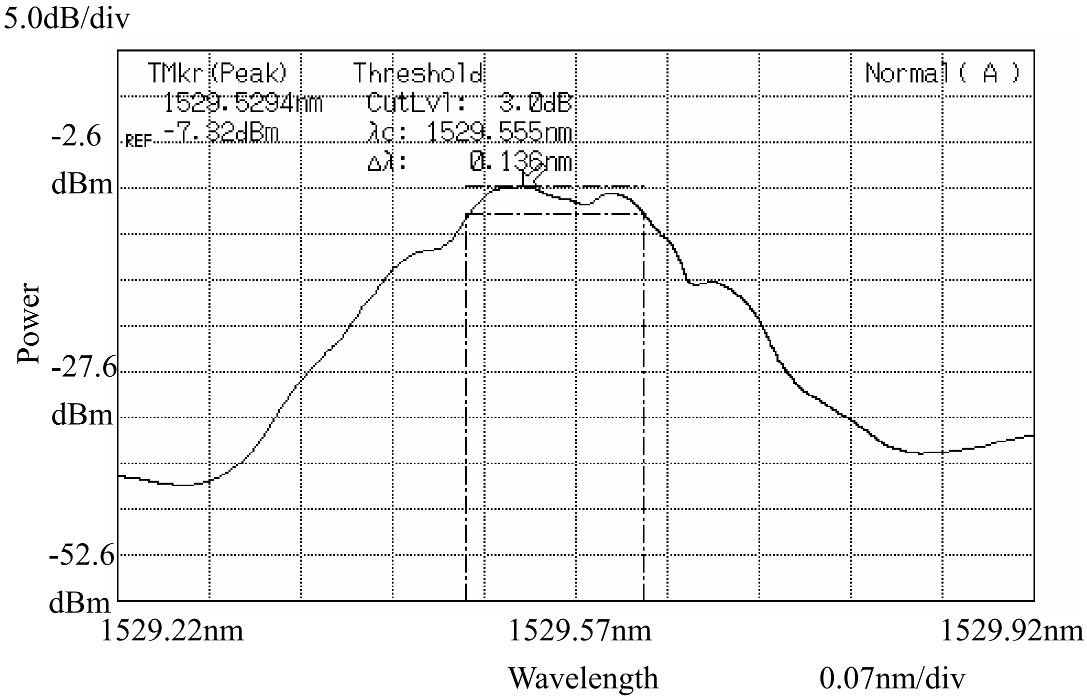


Fig. 2-22 Optical spectrum of RHMLFL with repetition rate of 10 GHz.

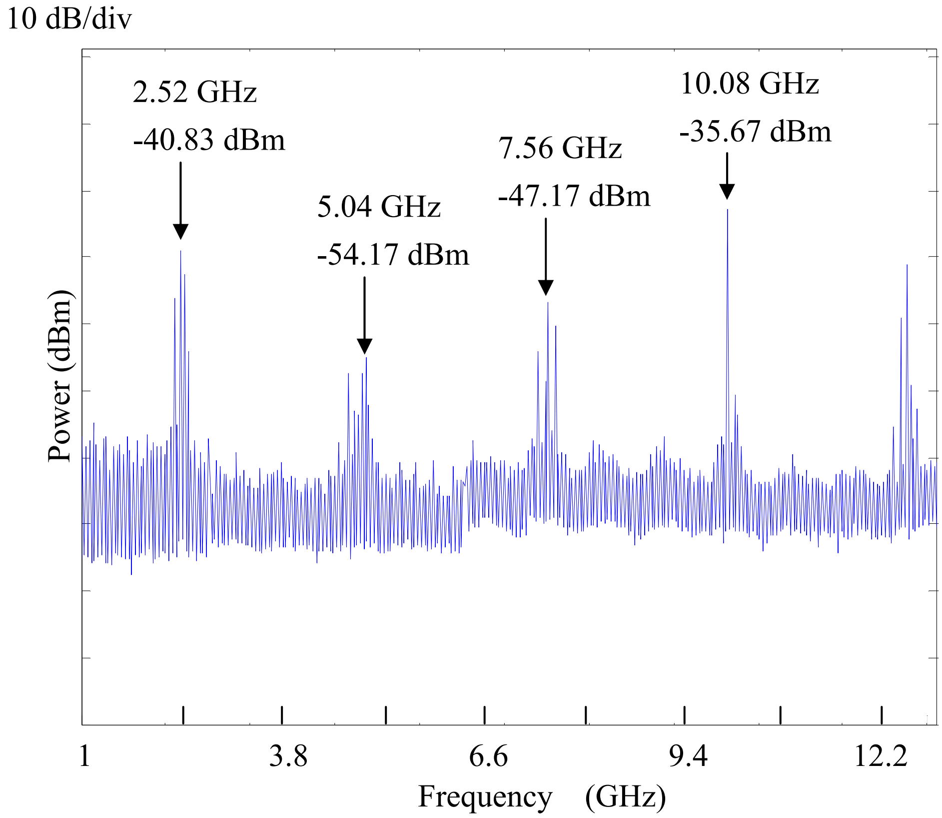


Fig. 2-23 RF spectrum(wideband) of RHMLFL with repetition rate of 10 GHz.

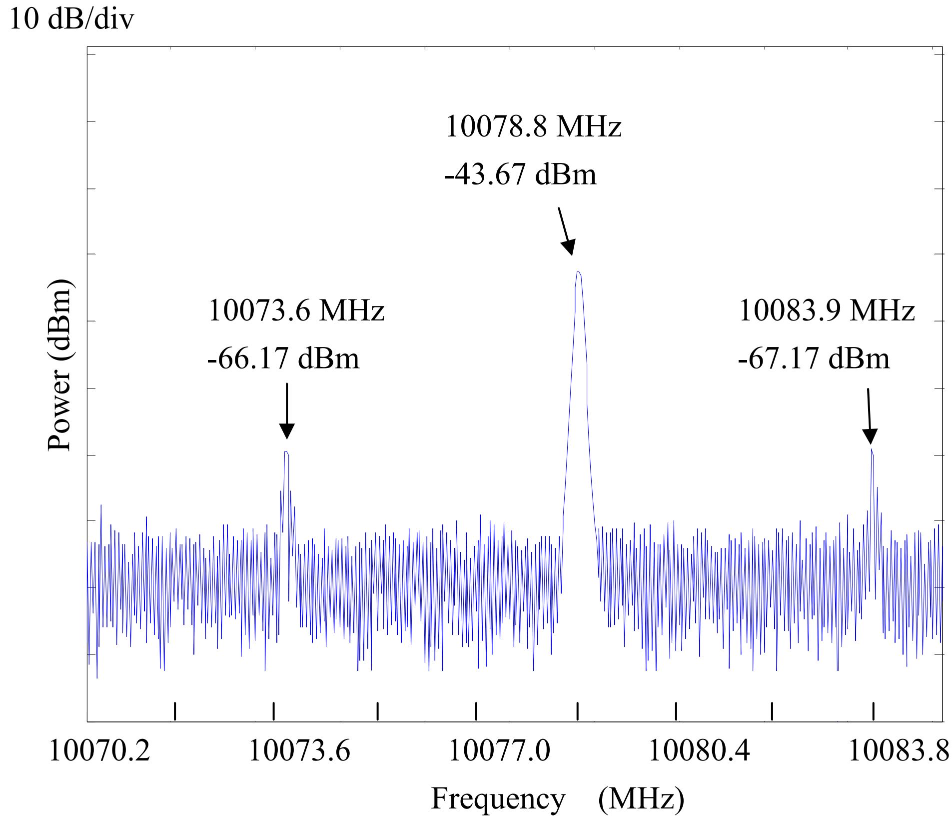


Fig. 2-24 RF spectrum(narrowband) of RHMLFL with repetition rate of 10 GHz.

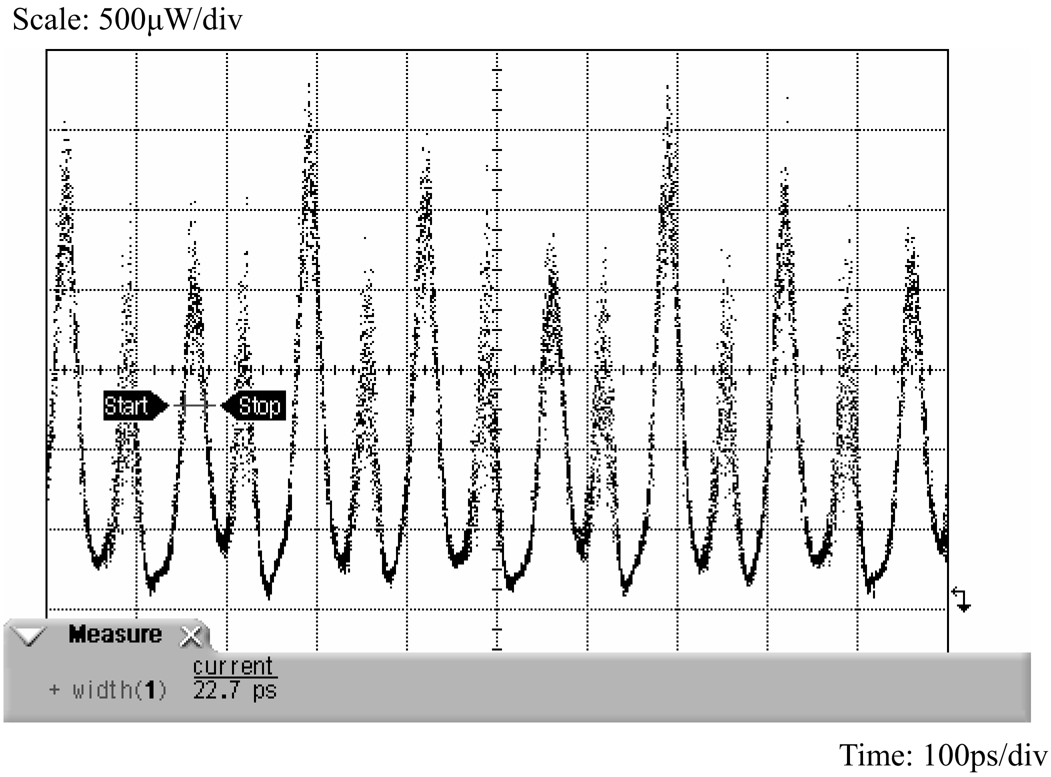


Fig. 2-25 Pulse train of RHMLFL with repetition rate of 15 GHz.

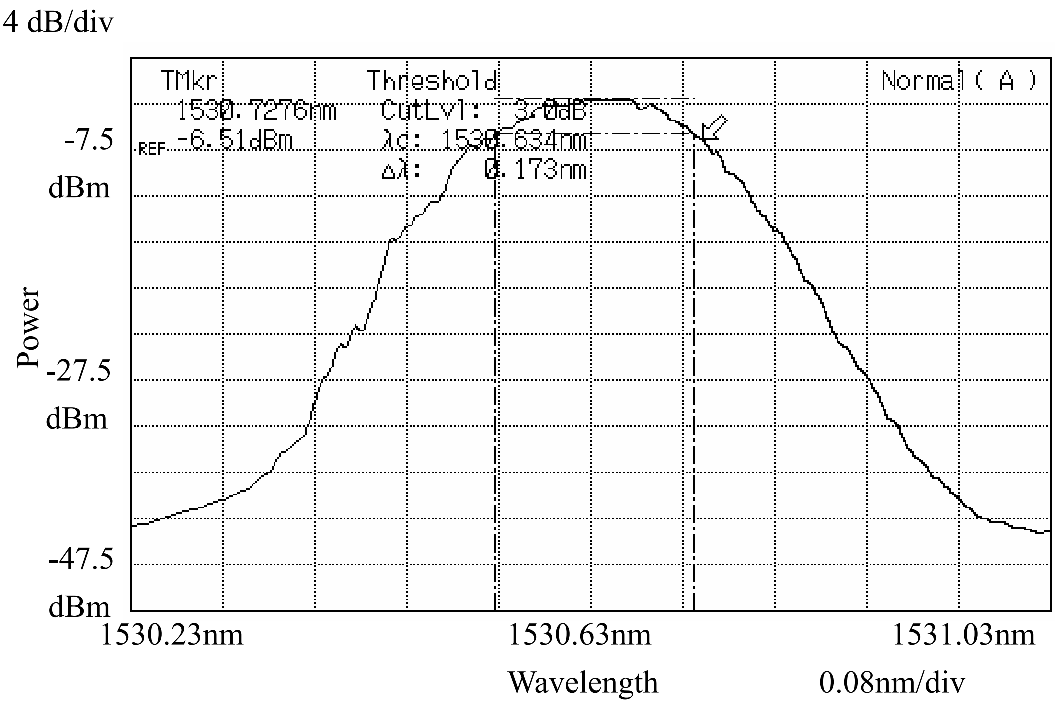


Fig. 2-26 Optical spectrum of RHMLFL with repetition rate of 15 GHz.

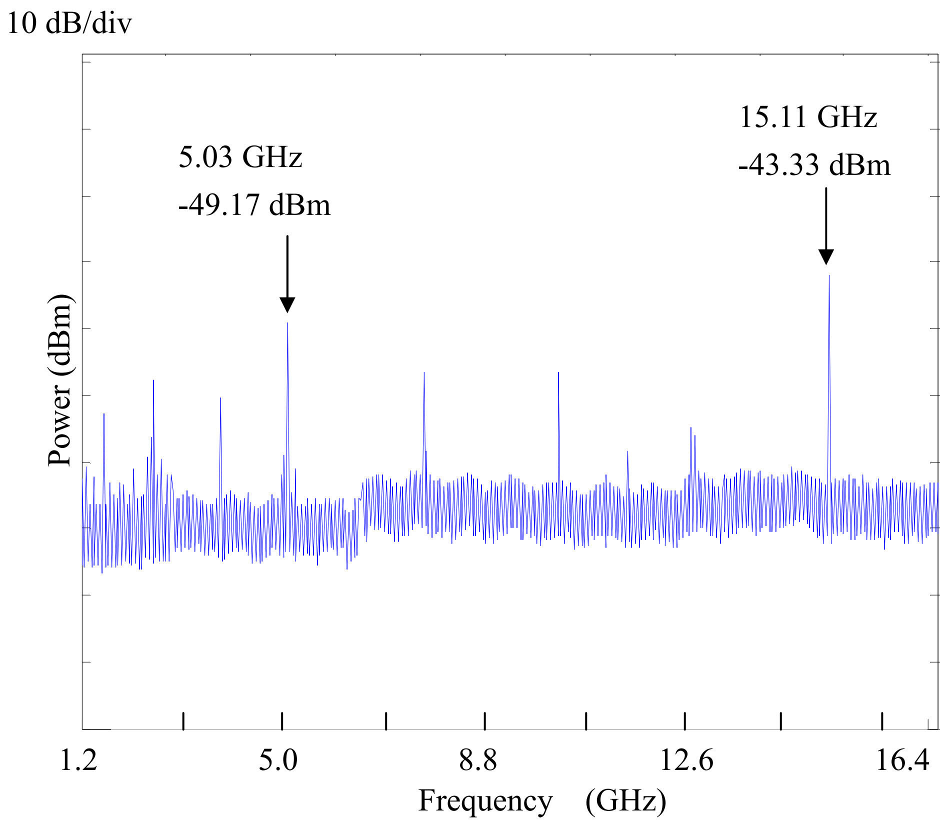


Fig. 2-27 RF spectrum(wideband) of RHMLFL with repetition rate of 15 GHz.

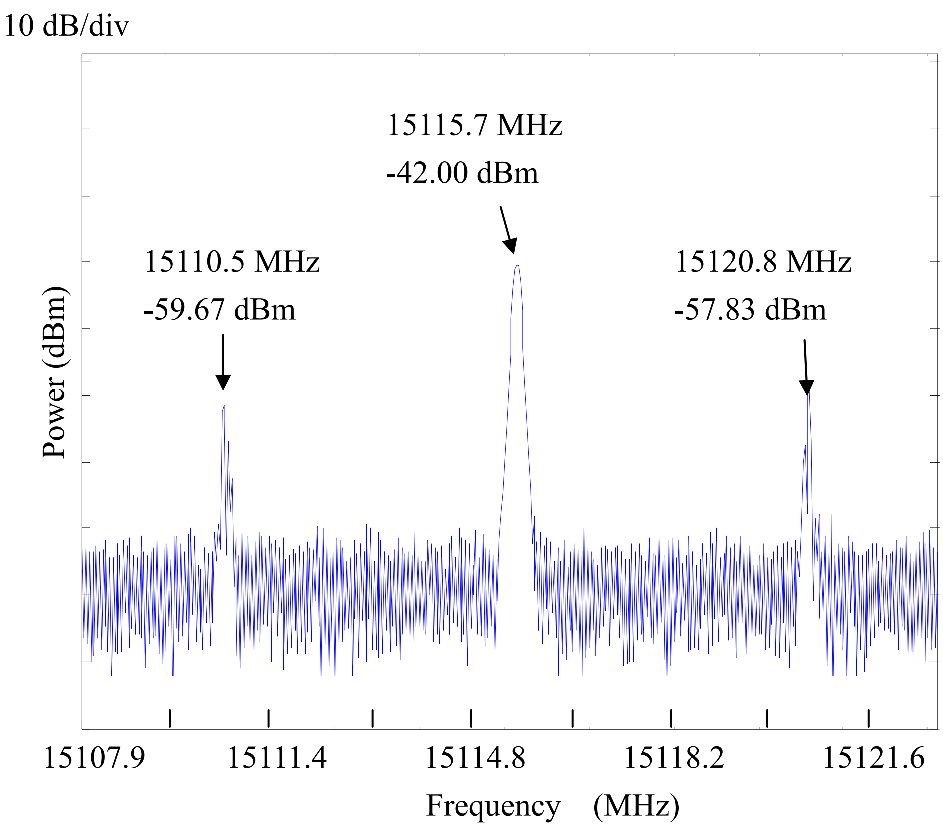


Fig. 2-28 RF spectrum(narrowband) of RHMLFL with repetition rate of 15 GHz.

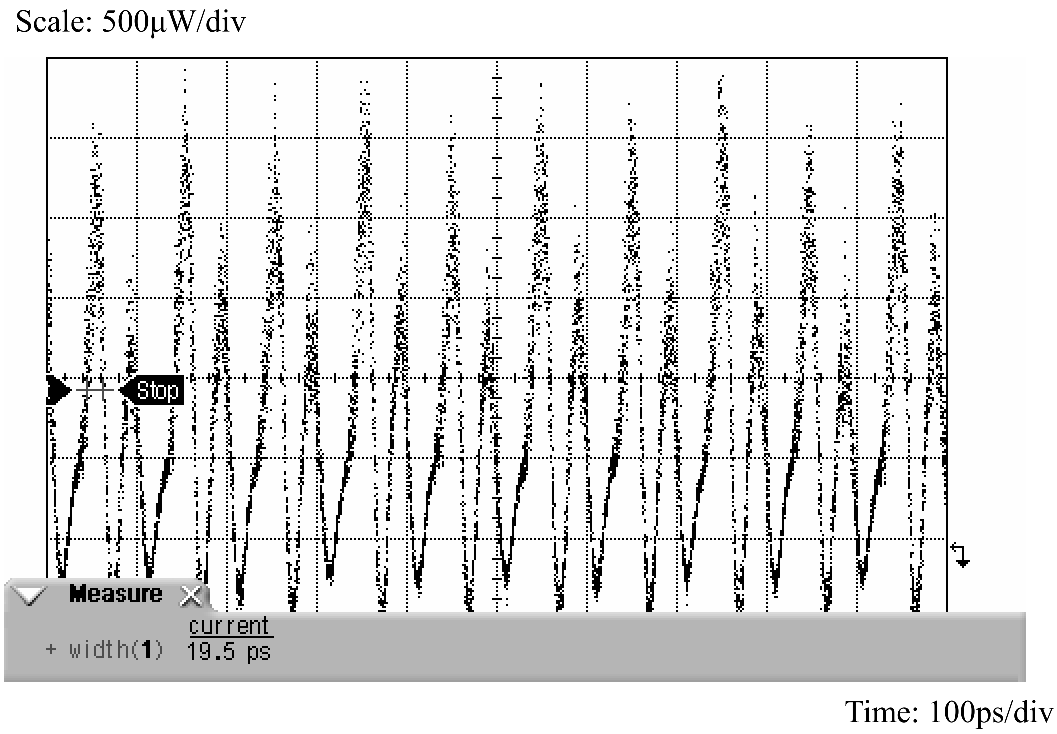


Fig. 2-29 Pulse train of RHMLFL with repetition rate of 20 GHz.

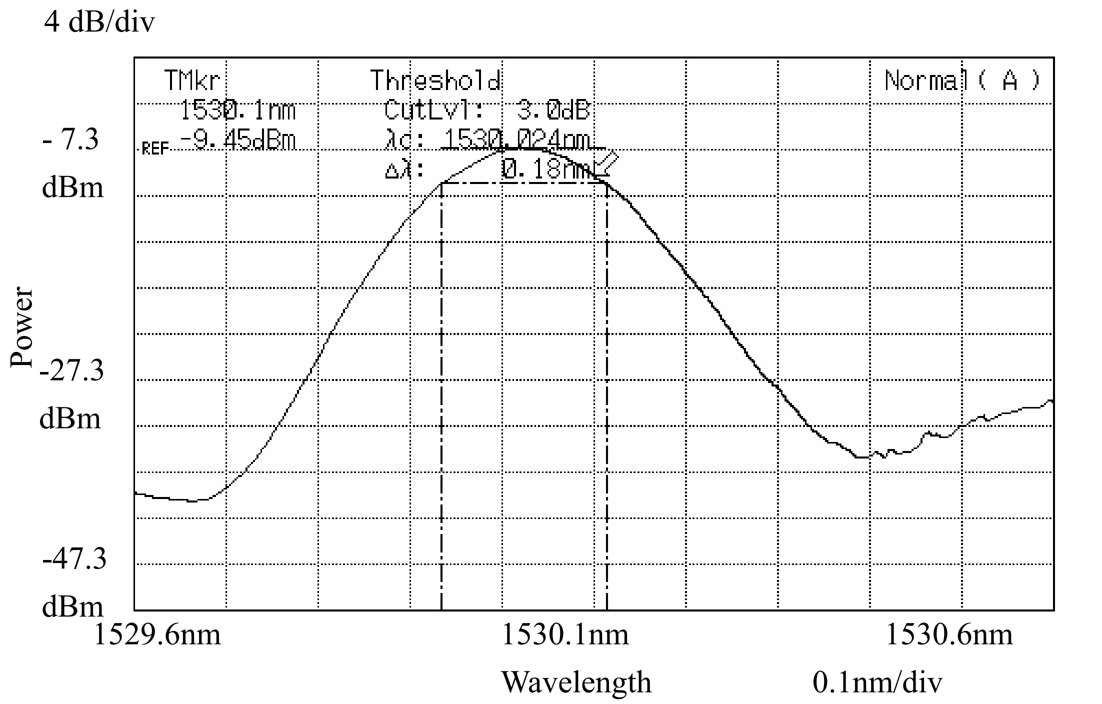


Fig. 2-30 Optical spectrum of RHMLFL with repetition rate of 20 GHz.

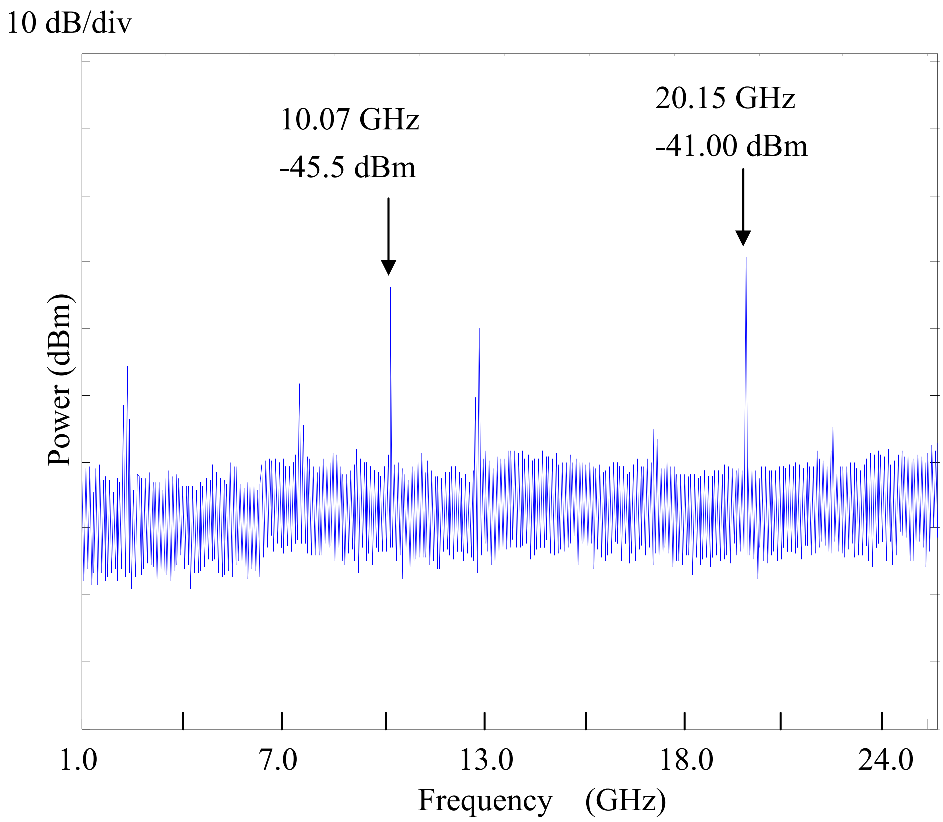


Fig. 2-31 RF spectrum(wideband) of RHMLFL with repetition rate of 20 GHz.

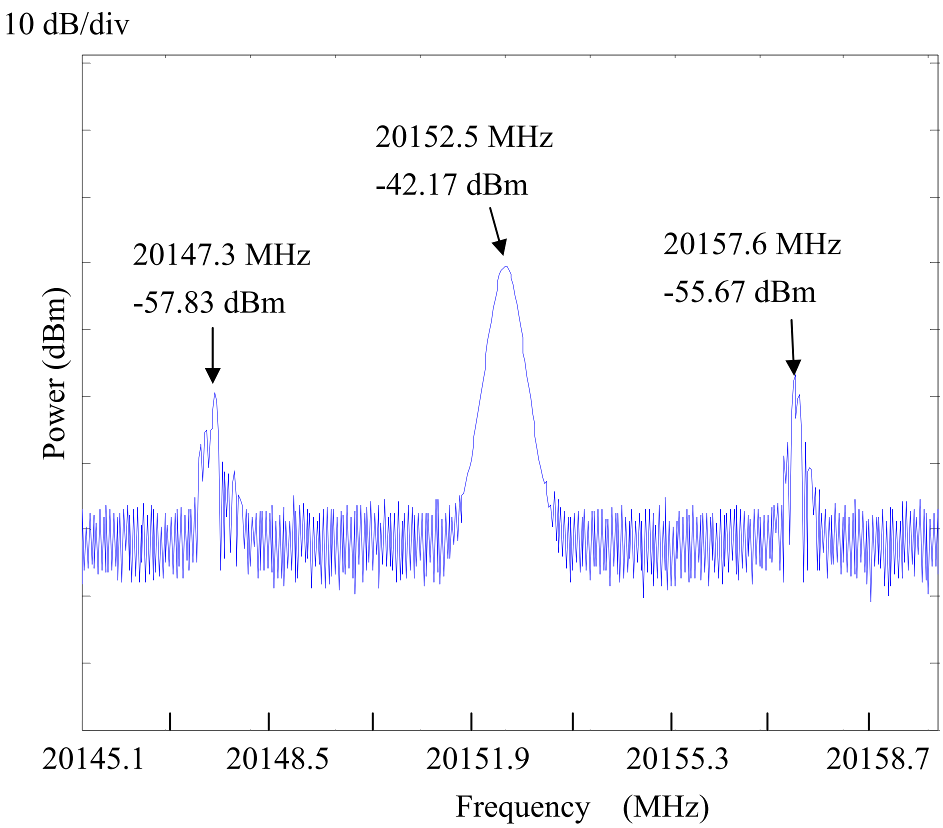


Fig. 2-32 RF spectrum(narrowband) of RHMLFL with repetition rate of 20 GHz.

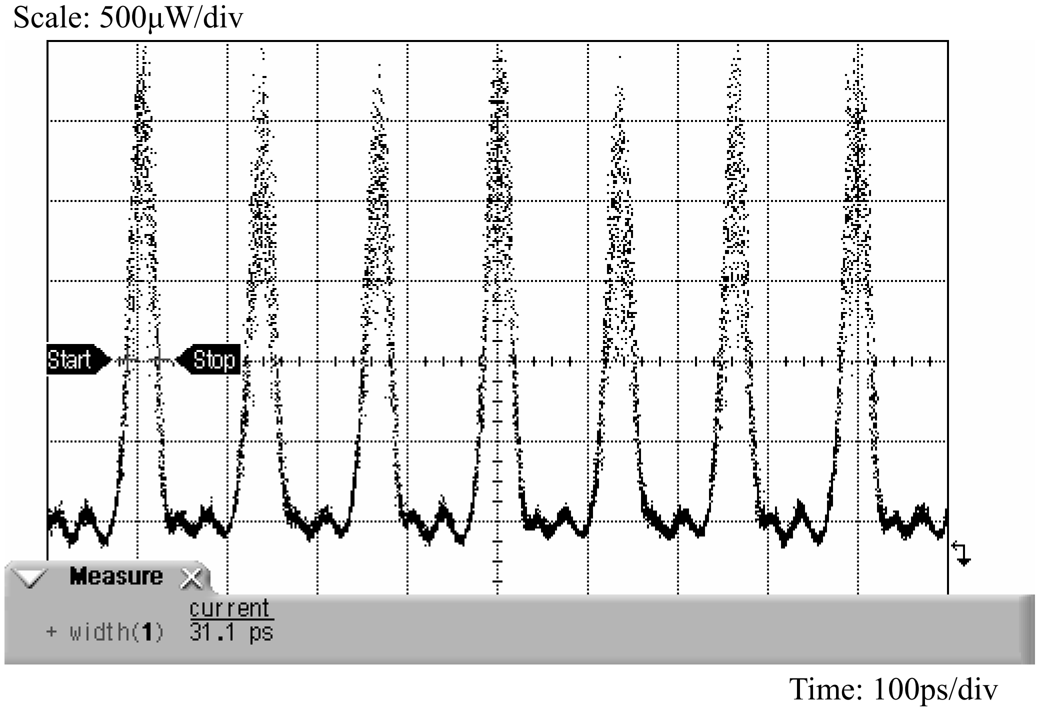

Fig. 2-33 Amplitude equalization of RHMLFL with repetition rate of 7.5 GHz.

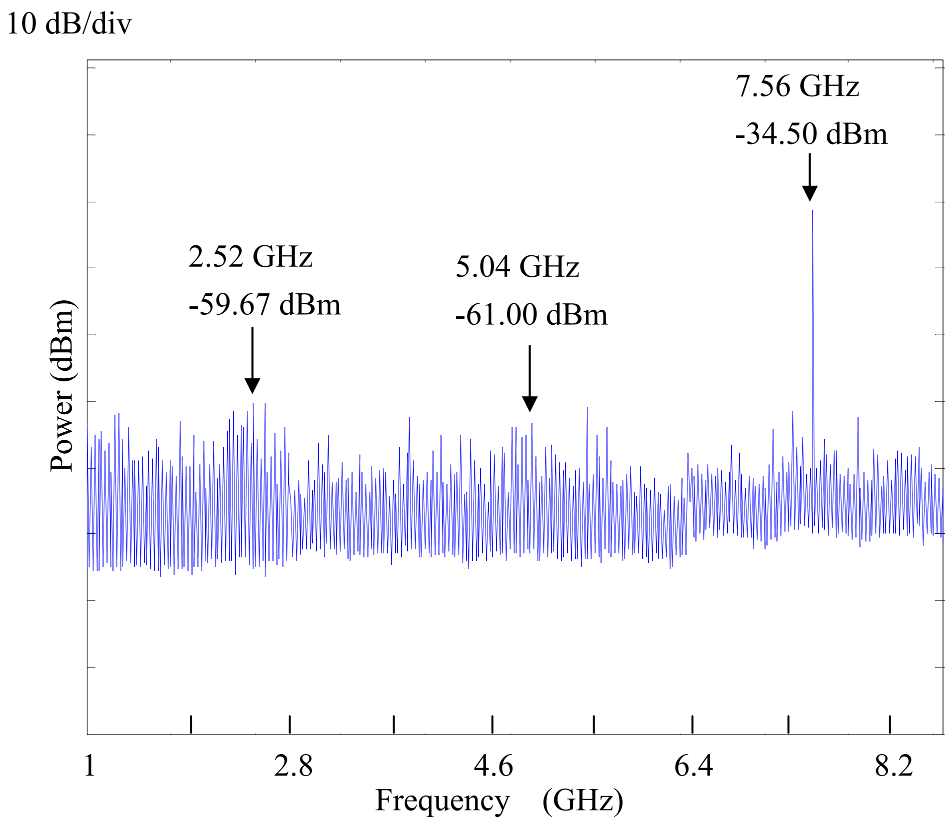

Fig. 2-34 RF spectrum of RHMLFL with repetition rate of 7.5 GHz with suppressed lower harmonics by nonlinear modulation.

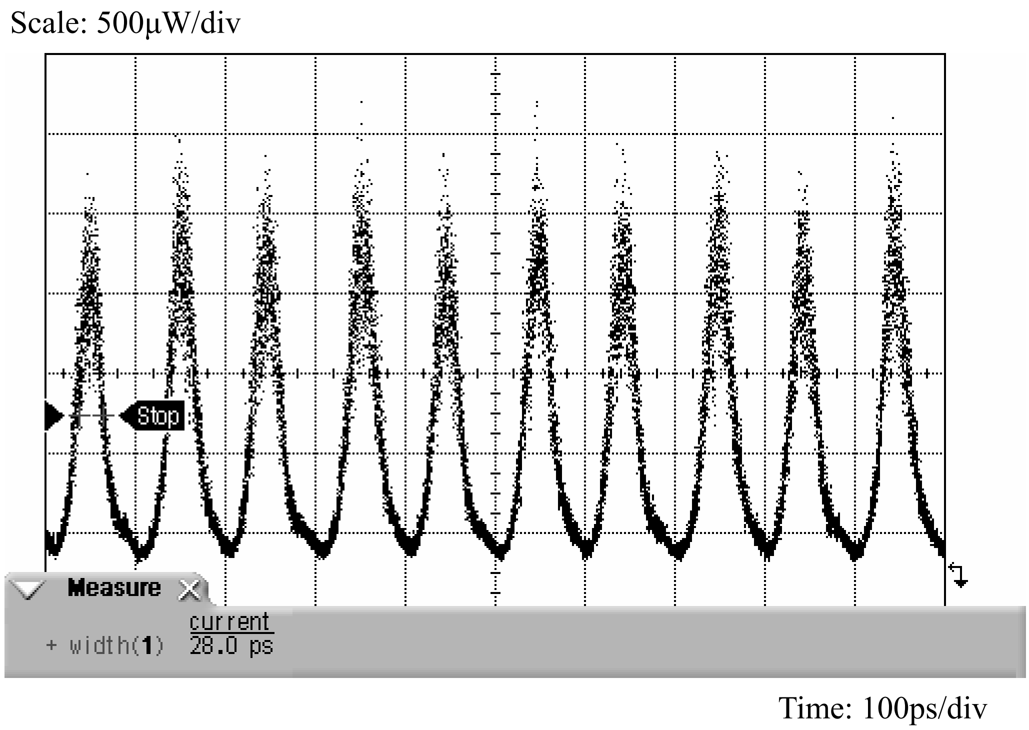


Fig. 2-35 Amplitude equalization of RHMLFL with repetition rate of 10 GHz.

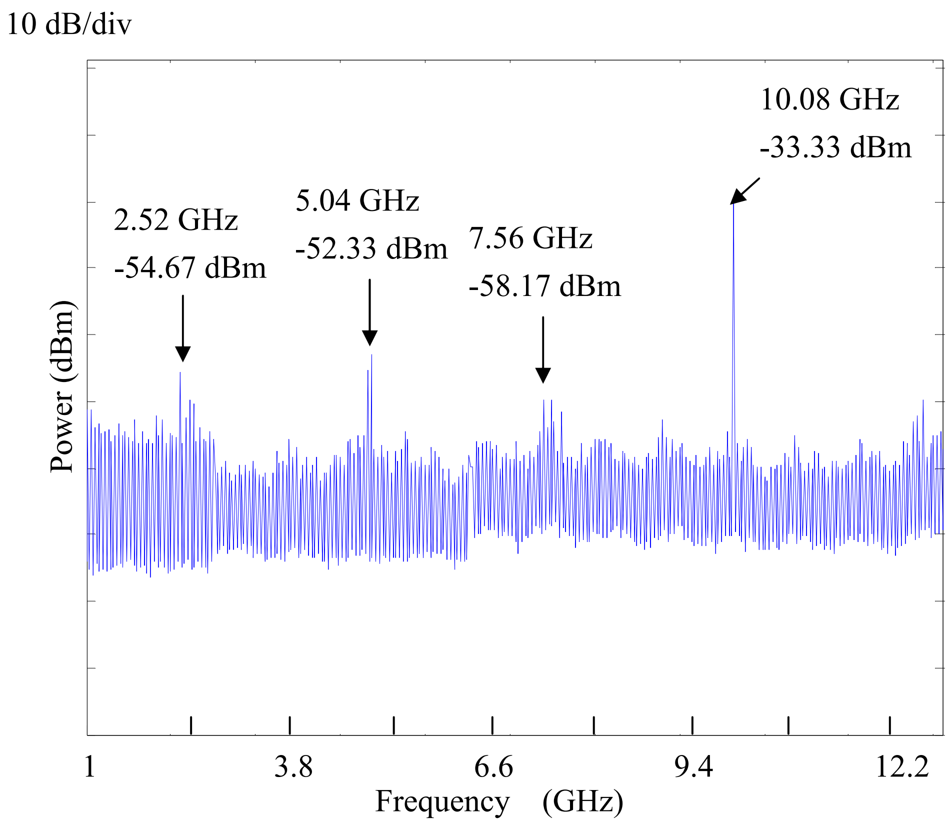


Fig. 2-36 RF spectrum of RHMLFL with repetition rate of 10 GHz with suppressed lower harmonics by nonlinear modulation.

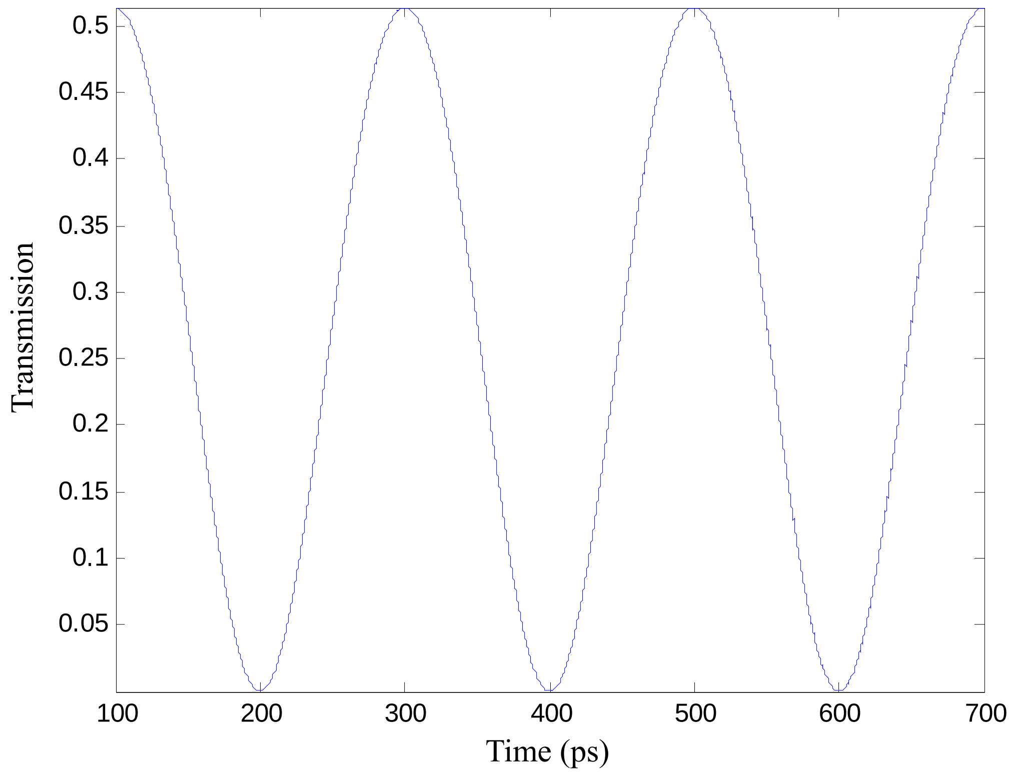


Fig. 2-37 Transfer function of the modulator when b=1.5 and M=0.42 for the fourth order rational harmonic mode locking.

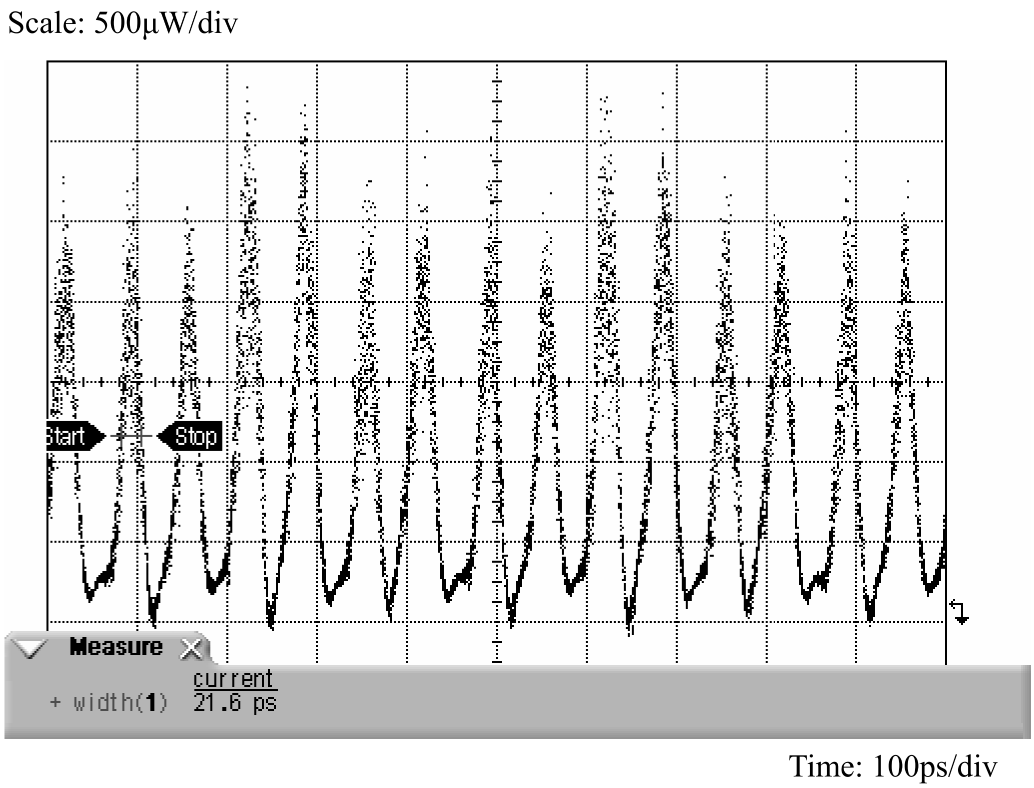


Fig. 2-38 Amplitude equalization of RHMLFL with repetition rate of 15 GHz.

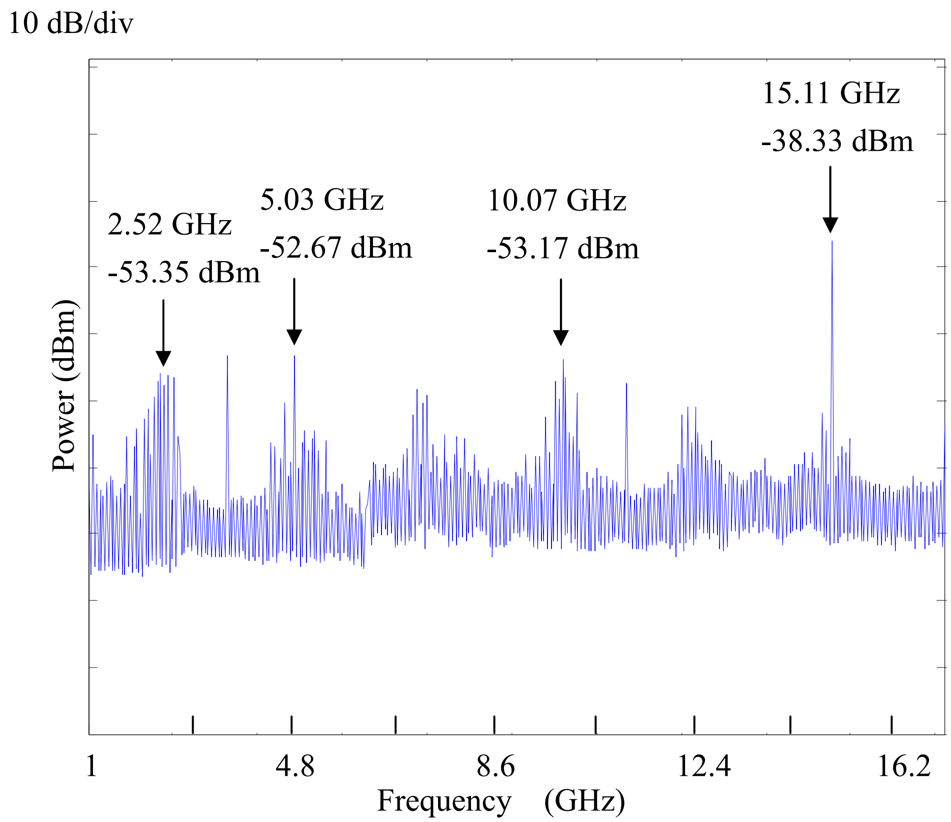


Fig. 2-39 RF spectrum of RHMLFL with repetition rate of 15 GHz with suppressed lower harmonics by nonlinear modulation.

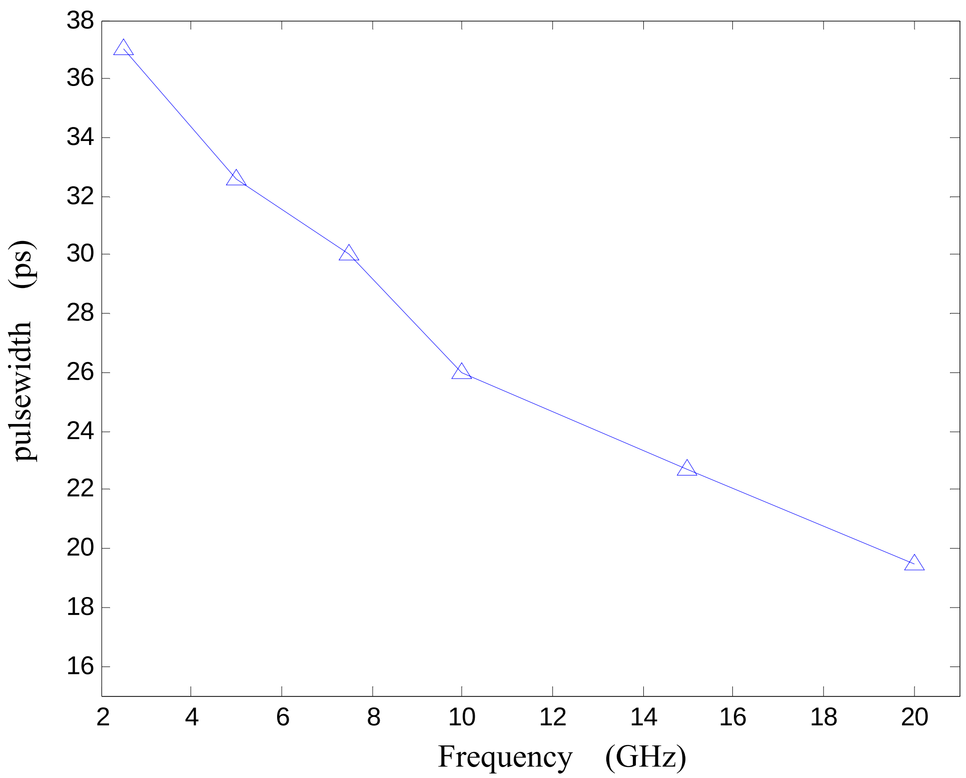


Fig. 2-40 Pulsewidth of RHMLFL for various repetition rates.

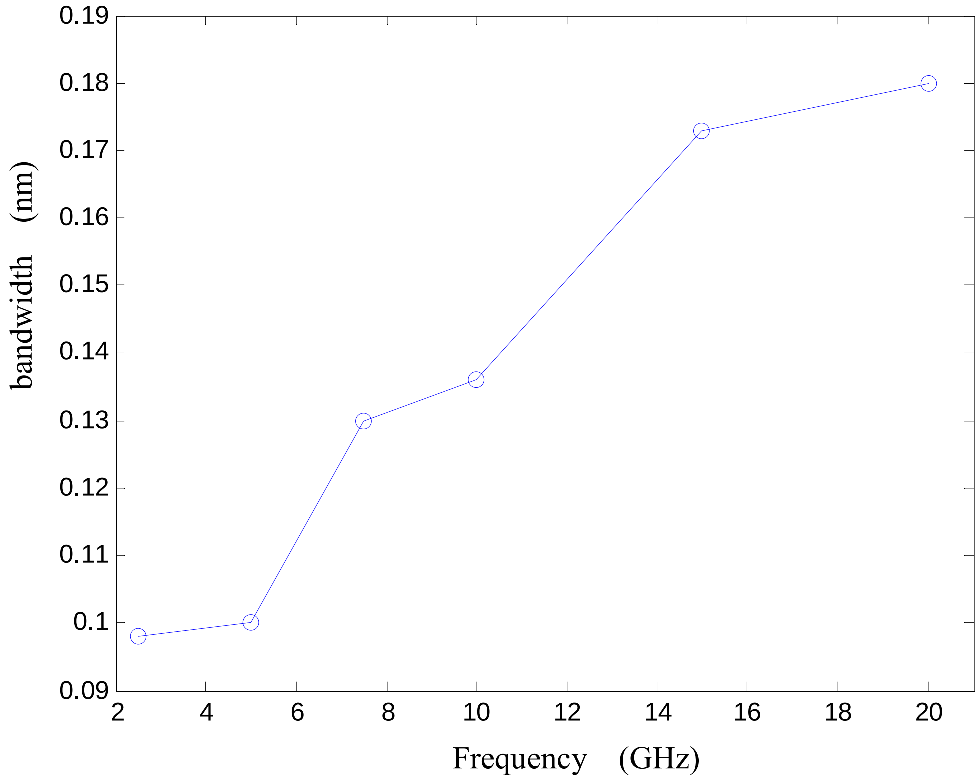


Fig. 2-41 Bandwidth of RHMLFL for various repetition rates.

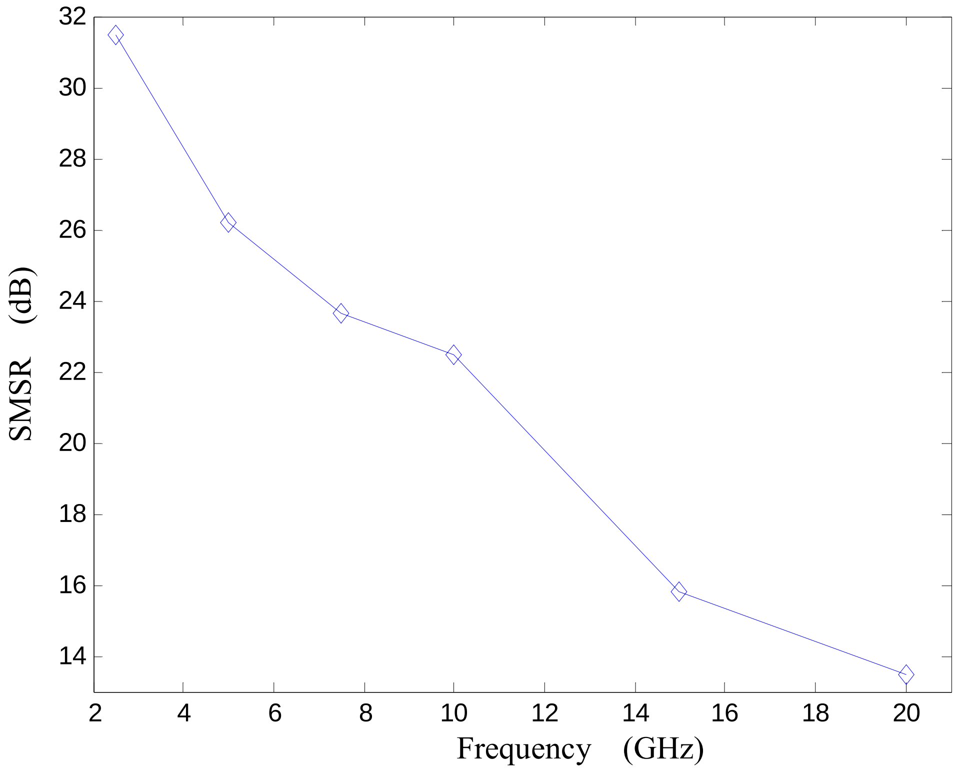


Fig. 2-42 SMSR of RHMLFL for various repetition rates.

Table. 2-1 MZI modulator transmission function measurement result

| $V_{bias}$(V) | -6 | -5.6 | -5.2 | -4.8 | -4.4 | -4.0 | -3.6 | -3.2 |
|---|---|---|---|---|---|---|---|---|
| $P_{out}$(dBm) | -6.85 | -6.30 | -6.05 | -5.95 | -6.05 | -6.35 | -6.80 | -7.50 |
| $P_{out}$(mW) | 0.206 | 0.234 | 0.248 | 0.254 | 0.248 | 0.232 | 0.209 | 0.179 |
| T | 0.785 | 0.891 | 0.944 | 0.966 | 0.944 | 0.881 | 0.794 | 0.676 |

| $V_{bias}$(V) | -2.8 | -2.4 | -2.0 | -1.6 | -1.2 | -0.8 | -0.4 | 0 |
|---|---|---|---|---|---|---|---|---|
| $P_{out}$(dBm) | -8.40 | -9.60 | -11.20 | -13.40 | -16.6 | -21.3 | -25.6 | -18.5 |
| $P_{out}$(mW) | 0.145 | 0.109 | 0.076 | 0.046 | 0.022 | 0.007 | 0.003 | 0.014 |
| T | 0.549 | 0.417 | 0.288 | 0.174 | 0.083 | 0.028 | 0.010 | 0.053 |

| $V_{bias}$(V) | 0.4 | 0.8 | 1.2 | 1.6 | 2 | 2.4 | 2.8 | 3.2 |
|---|---|---|---|---|---|---|---|---|
| $P_{out}$(dBm) | -14.70 | -12.05 | -10.2 | -8.7 | -7.7 | -6.5 | -6.30 | -5.95 |
| $P_{out}$(mW) | 0.033 | 0.062 | 0.095 | 0.135 | 0.169 | 0.224 | 0.234 | 0.254 |
| T | 0.129 | 0.237 | 0.363 | 0.513 | 0.646 | 0.851 | 0.891 | 0.966 |

| $V_{bias}$(V) | 3.6 | 3.8 | 4.0 | 4.4 | 4.8 | 5.2 | 5.6 | 6 |
|---|---|---|---|---|---|---|---|---|
| $P_{out}$(dBm) | -5.85 | -5.8 | -5.85 | -6.1 | -6.65 | -7.40 | -8.6 | -10.05 |
| $P_{out}$(mW) | 0.26 | 0.263 | 0.26 | 0.245 | 0.216 | 0.182 | 0.138 | 0.099 |
| T | 0.989 | 1 | 0.98 | 0.933 | 0.822 | 0.691 | 0.525 | 0.376 |